



Review Article

Origin and models of oceanic transform faults

Taras Gerya*

Swiss Federal Institute of Technology Zurich, Department of Geosciences, Zurich, Switzerland

ARTICLE INFO

Article history:

Received 22 March 2011

Received in revised form 30 June 2011

Accepted 7 July 2011

Available online 22 July 2011

Keywords:

Transform faults
Mid-ocean ridges
Analog models
Numerical models

ABSTRACT

Mid-ocean ridges sectioned by transform faults represent prominent surface expressions of plate tectonics. A fundamental problem of plate tectonics is how this pattern has formed and why it is maintained. Gross-scale geometry of mid-ocean ridges is often inherited from respective rifted margins. Indeed, transform faults seem to nucleate after the beginning of the oceanic spreading and can spontaneously form at a single straight ridge. Both analog and numerical models of transform faults were investigated since the 1970s. Two main groups of analog models were developed: thermomechanical (freezing wax) models with accreting and cooling plates and mechanical models with non-accreting lithosphere. Freezing wax models reproduced ridge–ridge transform faults, inactive fracture zones, rotating microplates, overlapping spreading centers and other features of oceanic ridges. However, these models often produced open spreading centers that are dissimilar to nature. Mechanical models, on the other hand, do not accrete the lithosphere and their results are thus only applicable for relatively small amount of spreading. Three main types of numerical models were investigated: models of stress and displacement distribution around transforms, models of their thermal structure and crustal growth, and models of nucleation and evolution of ridge–transform fault patterns. It was shown that a limited number of spreading modes can form: transform faults, microplates, overlapping spreading centers, zigzag ridges and oblique connecting spreading centers. However, the controversy exists whether these patterns always result from pre-existing ridge offsets or can also form spontaneously at a single straight ridge during millions of year of accretion. Therefore, two types of transform fault interpretation exist: plate fragmentation structures vs. plate accretion structures. Models of transform faults are yet relatively scarce and partly controversial. Consequently, a number of first order questions remain standing and significant cross-disciplinary efforts are needed in the future by combining natural observations, analog experiments, and numerical modeling.

© 2011 Elsevier B.V. All rights reserved.

Contents

1. Introduction	34
2. Key observations	35
3. Analog modeling of transform faults	36
3.1. Freezing wax models	36
3.2. Non-accreting analog models	41
4. Numerical modeling of transform faults	43
4.1. Models of stress and displacement distribution	43
4.2. Models of thermal structure and crustal growth	45
4.3. Models of nucleation and evolution	46
5. Future modeling prospective	51
6. Summary and conclusions	52
Acknowledgments	53
References	53

1. Introduction

Transform faults represent a distinct type of tectonic plate boundaries along which plates and plate segments are passing each other

* Tel.: +41 44 6336623.

E-mail address: taras.gerya@erdw.ethz.ch.

horizontally. These boundaries are known both on continents and in the ocean floor. Continental transform faults (such as San Andreas, North Anatolian and Dead Sea transform faults) are generally better known and studied due to their good accessibility and notable seismic activity directly affecting our life. In contrast, oceanic transform faults that are much more abundant on Earth are much less accessible and remain largely enigmatic in terms of their origin and evolution. Mid-ocean ridges (MOR) sectioned by these orthogonal transform faults represent one of the most prominent surface expressions of terrestrial plate tectonics at globally developed constructive (accreting) plate boundaries where the oceanic lithosphere is created. The perpendicularity of the ridges and the transform faults is so common that it is considered to be an “intrinsic property” of the oceanic spreading process (Oldenburg and Brune, 1972). Tens to hundreds of kilometer long active transform fault sections connecting two spreading centers are typically extended from both sides by even longer (up to thousands of kilometers) inactive fracture zones of similar orientation.

One common view is that both continental and oceanic transform faults have the same origin and result from plate fragmentation often controlled by pre-existing structures (e.g., Wilson, 1965; Cochran and Martinez, 1988; McClay and Khalil, 1998; Choi et al., 2008; Hieronymus, 2004). This view is, in particular, based on a geometric correspondence between passive margins and mid-ocean ridges, which is especially prominent for the South Atlantic Ridge and the West African coast. It is, therefore, commonly viewed that transform faults develop in regions adjacent to originally offset ridge segments and that these offsets remain constant through time (e.g., Choi et al., 2008; Hieronymus, 2004; Oldenburg and Brune, 1972). However, several lines of evidence from both analog models and nature contradict this common view and suggest that oceanic transform faults may nucleate spontaneously and that ridge offsets along the faults can change with time (e.g., Sandwell, 1986; Stoddard and Stein, 1988; Taylor et al., 2009).

From the mechanical point of view an important question is why the typical spreading direction-parallel orientation of the oceanic transform faults is so different compared to typical spreading direction-inclined orientation of strike-slip shear zones that control plate fragmentation pattern under extension (e.g., Chemenda et al., 2002). To explain the peculiar orthogonal ridge-transform-fault pattern thermal stresses in cooling oceanic plates are often referred to as modifying stress distribution at MOR and thus changing fault orientation during oceanic plate fragmentation processes (e.g., Choi et al., 2008 and references therein). In addition, it is suggested that the transform faults should be rheologically very weak compared to the plates themselves in order to preserve the orthogonal pattern during the ongoing plate separation (e.g., Behn et al., 2002; Oldenburg and Brune, 1972). The orthogonality between ridge axes and transform faults was also explained by the principle of least-energy dissipation in the plastic flow at diverging plate boundaries; on the basis of a simple analytical model it was suggested that this geometry implies the existence of a narrow vertical injection channel under oceanic ridges that control most of energy dissipation (Froidevaux, 1973).

A fundamental long standing problem of plate tectonics is how the orthogonal ridge transform fault pattern typical of spreading oceanic ridges has formed and why it is maintained. The large time scales involved in the evolution of this pattern on the Earth prohibit real time observation. Consequently, the orthogonal ridge-transform fault pattern remained captivating for Earth scientists for decades with new data and ideas stemming from natural observations as well as from analog and numerical modeling. The two last methods are essential for understanding dynamics of MOR and transform faults since the natural record only provides integrated snapshot pictures resulting from millions and tens of millions of years of plate separation. It should, however, be mentioned that in contrast to observational studies of oceanic transform faults both analog and numerical modeling of these structures are yet much less systematic. This is especially obvious in comparison with a large amount of

models investigated for other key geodynamic processes, such as mantle convection, oceanic subduction, continental collision and lithospheric extension.

In this paper I will review key natural observations and results from analog and numerical modeling aimed to decipher the origin, structure and orientation of oceanic transform faults. I will also outline possible future directions for better understanding these crucial structural features of terrestrial plate tectonics.

2. Key observations

Mid-ocean ridge-transform fault pattern in nature varies as a function of spreading rate; this has been the subject of several reviews and systematics (e.g., Choi et al., 2008; Dick et al., 2003; Gudmundsson, 2007; Kriner et al., 2006; Macdonald et al., 1991; Menard, 1967; Rundquist and Sobolev, 2002; Sandwell, 1986; Small, 1998). Mid-ocean ridges have been divided into fast-, intermediate-, and slow-spreading, each with distinctive morphologic characteristics (e.g., Dick et al., 2003; Kriner et al., 2006; Small, 1998). Slow-spreading ridges (less than 50 mm/yr full spreading rate) have deep rift valleys with highly variable relief from ~400 to 2500 m and rough rift mountain topography weakly correlated to spreading rate. Fast-spreading ridges (80–180 mm/yr) have low (~400 m) axial highs, sometimes with small linear depressions (less than ~100 m wide and less than ~10 m deep) at their crests, and minimal rift mountain topography uncorrelated to spreading rate. Intermediate spreading ridges (~50–80 mm/yr) have long alternating sections with either slow- or fast-spreading ridge morphology (e.g., Dick et al., 2003; Kriner et al., 2006; Small, 1998). Dick et al. (2003) proposed discriminating ultraslow spreading ridges (less than 12–20 mm/yr) consisting of linked magmatic and amagmatic accretionary ridge segments. Recently, Kriner et al. (2006) demonstrated that ultrafast (more than 120 mm/yr) spreading ridges can also be distinguished based on peculiar abyssal hill morphology.

Tectonic processes at mid-ocean ridges are affected by spreading rates (e.g., Buck et al., 2005; Escartin et al., 2008; Kriner et al., 2006 and references therein). In particular, the formation of oceanic detachment faults that are often associated with asymmetric accretion is well established along ridges spreading at less than 80 mm/yr (e.g., Allerton et al., 2000; Collier et al., 1997; Escartin et al., 2008 and references therein). On the other hand, transform faults are found in all above mentioned types of ridges, ultraslow ones excepted (Dick et al., 2003). Also, according to study of Naar and Hey (1989) oceanic transform faults with slip rates greater than ~145 mm/yr do not currently exist along the East Pacific Rise where sea-floor spreading rates range from 145 to 160 mm/yr. Instead, offsets of the very fast spreading East Pacific Rise are accommodated by microplates, propagating rifts, or overlapping spreading centers. This suggests that there might also be an upper spreading rate limit above which transform faults do not exist.

The crustal structure and gravity signature in the regions of transform faults change with changing spreading rate of the ridge (e.g., Gregg et al., 2007 and references therein). Slow-spreading mid-ocean ridge segments exhibit significant crustal thinning towards transform and non-transform offsets (Blackman and Forsyth, 1991; Kuo and Forsyth, 1988; Lin et al., 1990; Lin and Phipps Morgan, 1992; Tolstoy et al., 1993), which is thought to arise from a three-dimensional process of buoyant mantle upwelling and melt migration focused beneath the centers of ridge segments (e.g., Blackman and Forsyth, 1991; Kuo and Forsyth, 1988; Lin et al., 1990; Lin and Phipps Morgan, 1992). In contrast, fast-spreading mid-ocean ridges are characterized by smaller, segment-scale variations in crustal thickness, which possibly implies rather uniform mantle upwelling beneath the ridge axis (Canales et al., 2003; Fox and Gallo, 1984; Macdonald et al., 1988). Accordingly, a strong correlation exists between gravity signature of transform faults and spreading rate: slow-slipping transform faults are marked by gravity anomalies more positive than the adjacent ridge segments (e.g., Kuo and Forsyth, 1988; Lin et al., 1990; Lin and Phipps Morgan, 1992);

conversely, intermediate and fast-slipping transform faults exhibit gravity anomalies more negative than the adjacent ridge segments (Gregg et al., 2007). This indicates that there is a mass deficit at intermediate and fast-slipping transform faults, which could reflect increased rock porosity, serpentinization of mantle peridotite and/or crustal thickening (Gregg et al., 2007). The most negative anomalies correspond to topographic highs flanking the transform faults, rather than to transform troughs, presumably indicating that magmatic crustal thickening may take place at the flanks of transforms at faster spreading rates (Gregg et al., 2007, 2009).

Transform faults are seismically active plate boundaries (e.g., Brune, 1968; Rundquist and Sobolev, 2002) but how they slip remains poorly understood (e.g., Abercrombie, and Ekström, 2001). There is a clear difference in seismic regime between transform faults and spreading centers (e.g., Rundquist and Sobolev, 2002 and references therein). The first have seismic moment release one-two orders higher; their contribution into the total seismic budget of mid ocean ridges increases with higher spreading rate. The relationships between the seismic moment release, fault length and spreading rate are quite different for transform and rift parts of MOR. Indeed, in both cases, the principal factor controlling the ridge seismicity is the thermal structure of the lithosphere (e.g., Rundquist and Sobolev, 2002). Several studies suggested that relatively slow earthquake rupture might be common for oceanic transform faults (e.g., Boettcher and Jordan, 2004; Kanamori and Stewart, 1976; Okal and Stewart, 1992) and that very slow slip precedes some oceanic transform earthquakes (e.g., Ihmle et al., 1979; Ihmle and Jordan, 1994; McGuire et al., 1996). Other studies suggest, however, that some slow precursors can be explained as artifacts of uncertainties in the assumed model parameters (e.g., Abercrombie, and Ekström, 2001). Boettcher and Jordan (2004) constructed scaling relations for the seismicity of oceanic transforms and concluded that about 85% of the slip at the temperature less than 600 °C is accommodated by subseismic mechanisms such as steady aseismic creep, silent earthquakes, and infraseismic (quiet) events. These authors also speculated that the seismogenic stresses on ridge transform faults may be primarily regulated by slow transients, rather than the fast ruptures that dominate continental strike-slip faults. In this view, ordinary (loud) earthquakes on oceanic transforms would simply be “aftershocks” of quiet or silent events (Boettcher and Jordan, 2004).

The origin of transform faults remains in part enigmatic. On the one hand, the geometric coincidence between passive margins and the orthogonal pattern of ridges and transform faults led Wilson (1965) to propose that transform faults are inherited from preexisting structures. Later observations supported this idea by showing that stepping half-grabens (e.g., Cochran and Martinez, 1988; McClay and Khalil, 1998), segmented gravity and magnetic anomalies (e.g., Behn and Lin, 2000), or segmented weak regions (e.g., Watts and Stewart, 1998) along passive margins lead to the formation of transform faults found at respective mid-ocean ridges. On the other hand, a number of observations support the hypothesis that the orthogonal ridge-transform pattern can be emergent and is not solely due to preexisting structures (e.g., Menard and Atwater, 1968; Merkur'ev et al., 2009; Sandwell, 1986; Taylor et al., 2009).

Sandwell (1986) discussed several observations indicating that transform faults are inherent to the spreading process and not just inherited from initially curved plate boundaries.

- First evidence is that transform faults can spontaneously form at a single straight ridge, particularly after changes in the spreading direction (e.g., Menard and Atwater, 1968; Merkur'ev et al., 2009). For example, south of the Mendocino fracture zone, in the late Cretaceous, an orthogonal ridge-transform pattern developed from an initially long straight segment of spreading ridge (Winterer, 1976).
- Second evidence is the existence of zero offset transforms (zero offset fracture zones) discovered by Shouten and White (1980) in

the seafloor southwest of Bermuda. These structures may imply, in particular, notable changes of ridge offsets along transform faults with time due to asymmetric plate accretion (e.g., Stoddard and Stein, 1988).

- Third evidence is the correlation between length of ridge segment and spreading rate (e.g., Fox and Gallo, 1984; Sandwell, 1986) that cannot be explained with inherited transform fault structures.

In addition, Taylor et al. (2009) demonstrated that data from the Woodlark Basin, Gulf of Aden and NW Australia suggest that spreading segments nucleate en echelon in overlapping rift basins and that transform faults develop while or after oceanic spreading starts; typically these faults are not inherited from transverse rift structures. Initial offsets of spreading centers, where present, are often non-transform. Also, after continental break-up, spreading center segmentation is often modified by ridge jumps and/or propagation (Taylor et al., 2009).

In general, key observations are intriguing and require an adequate explanation: on the one hand, gross-scale geometries of mid-ocean ridge – transform fault patterns are often inherited from the respective rifted margins, on the other hand, transform faults themselves seem to nucleate after the beginning of the oceanic spreading and not during the continental breakup itself. Moreover, perpendicularity of mid-ocean ridges and transform faults contradicts mechanically favorable orientations of strike-slip faults forming during plate fragmentation under extension.

3. Analog modeling of transform faults

Since early 1970s, two main groups of analog models of transform faults were investigated: thermomechanical (freezing wax) models with accreting and cooling plates and mechanical models with non-accreting brittle lithosphere.

3.1. Freezing wax models

Analog modeling of transform faults started from the seminal work of Oldenburg and Brune (1972, 1975) who performed a series of freezing wax experiments (Fig. 1) to reproduce the orthogonal ridge-transform pattern of oceanic plate separation. In this thermomechanical analog model (Fig. 1a) a tray of melted paraffin was cooled by a variable-speed fan until a film of solidified wax formed between one end of the pan and a movable stick. The stick was drawn at a uniform rate through the wax by a variable-speed motor. In most cases a zone of weakness of arbitrary shape was predetermined to ensure that spreading did not initiate at the boundary of the stick. However, the characteristic ridge-transform fault pattern evolved even when this was not done (Oldenburg and Brune, 1972).

These laboratory experiment showed that ridge–ridge transform faults, inactive fracture zones and other feature characteristic of spreading oceanic ridges (Fig. 1b) can be produced in a variety of paraffins. Although the resultant pattern depends upon the temperature of the wax and the ratio of spreading rate to surface cooling, the characteristic orthogonal ridge-transform fault system is a preferred mode of separation. Symmetric spreading occurs under conditions of no tensile strength across the ridge, and the stability of transform faults is a consequence of their lack of shear strength. The experiments also showed that property characteristic of oceanic ridges occur under conditions of passive upwelling of material at the ridge crest controlled by the imposed plate separation and not by the active thermal convection (Oldenburg and Brune, 1972).

Interestingly, not all paraffins were able to produce transform faults. Oldenburg and Brune (1972) investigated a variety of paraffins with melting temperatures ranging from 55.5 °C to 69 °C: Shell 120 (melting point, 55.50 °C), Shell 200 (melting point, 62.8 °C), and Chevron 156 (melting point, 69 °C). Most successful experiments (and

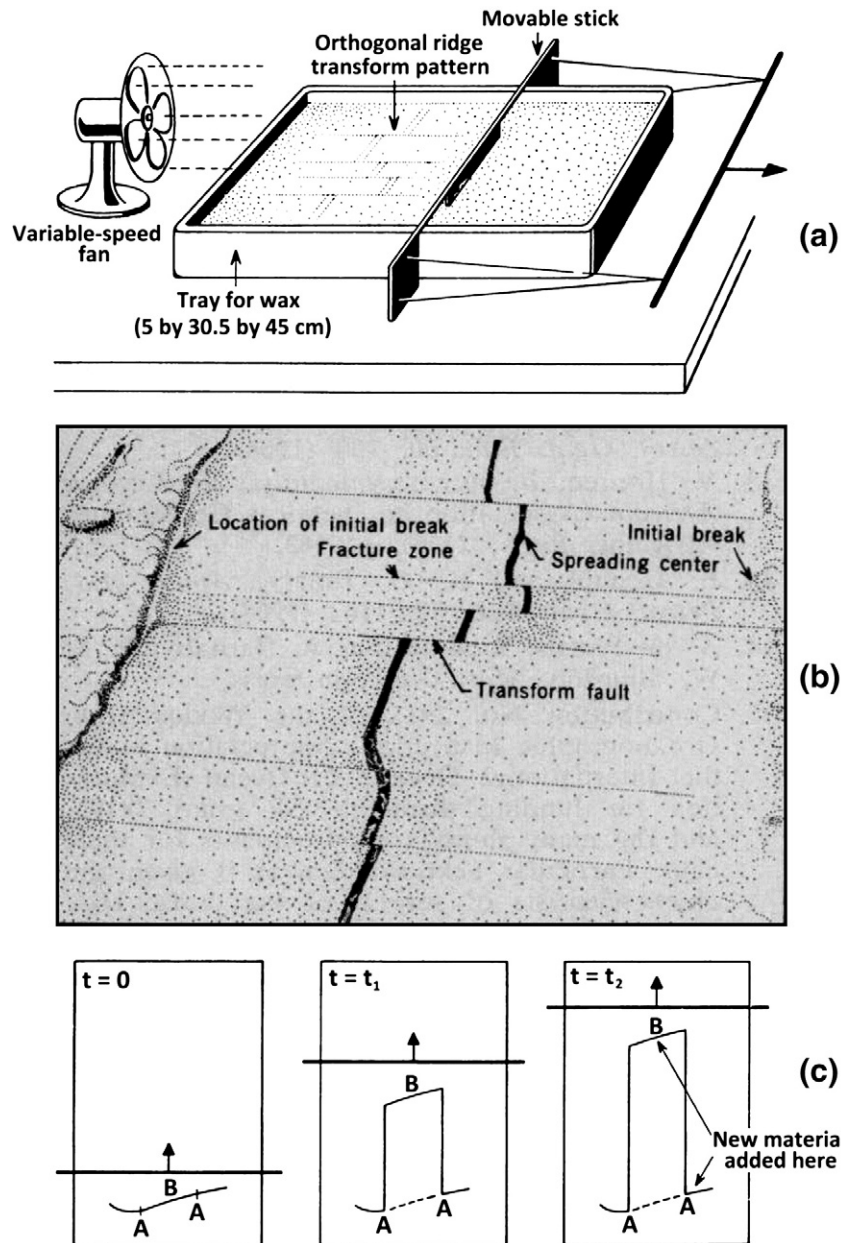


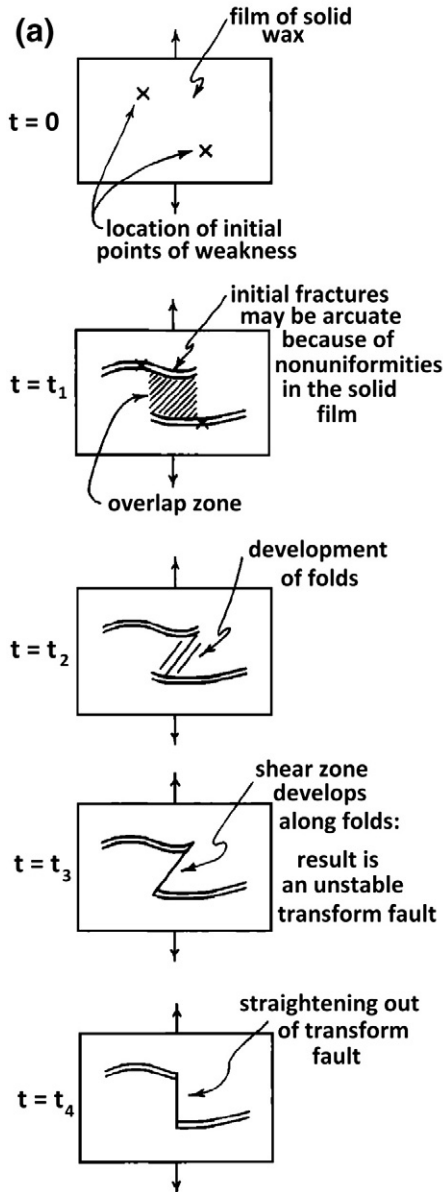
Fig. 1. Freezing wax experiment of Oldenburg and Brune (1972): (a) model setup, (b) typical experimental result, (c) spontaneous growth of transform faults by asymmetric plate accretion.

all documented photographs) were obtained with the use of Shell 120 wax. Other paraffins displayed similar patterns, although greater difficulty was encountered in obtaining the characteristic ridge transform fault pattern in Chevron 156 wax. Beeswax, a substance often used in geophysical modeling, did not produce transform faults (Oldenburg and Brune, 1972). In their later paper, Oldenburg and Brune (1975) demonstrated that the ability of various paraffin waxes to develop and maintain the orthogonal ridge-transform faults configuration can be characterized by the dimensionless ratio of the shear strength of the solid wax to the resistive stresses along the transform fault; the orthogonal pattern is maintained only when this ratio is greater than one. If this criterion is satisfied, the development of the orthogonal pattern is determined by the symmetry of the stress field and the ability of the wax to fracture in a brittle manner under these applied stresses. Freund and Merzer (1976) investigated microstructures of the wax crusts formed in analog models with transform faults similar to Oldenburg and Brune (1972) experiments. These crusts appeared to be composed of a warp yarn of wax fibers

with optical anisotropy. This fabric is absent in materials that fail to produce transform faults. Freund and Merzer (1976) suggested that the mechanical anisotropy of these wax films (with high tensile strength and low shear strength in the direction of spreading) is responsible for the initiation of the transform faults. They further suggested that the seismic anisotropy of the oceanic upper mantle may likewise be responsible for the creation of the ridge-ridge transform faults in the oceans (Freund and Merzer, 1976).

Oldenburg and Brune (1975) described in more details the process of formation of individual transform faults. According to their observations, transform faults nucleated after a thin film of the solidified wax was subjected to an extension at a uniform rate. As strain in the region increases, small openings occurring at random points of weakness in the solid plate act as starting locations for fractures that propagate outward in a brittle manner. The propagation of these cracks continues until the accumulated strain energy has been relieved, and the final configuration (Fig. 2a) often exhibits a small zone of overlap between the two ends of the newly formed

Formation of transform fault



Destruction of transform fault

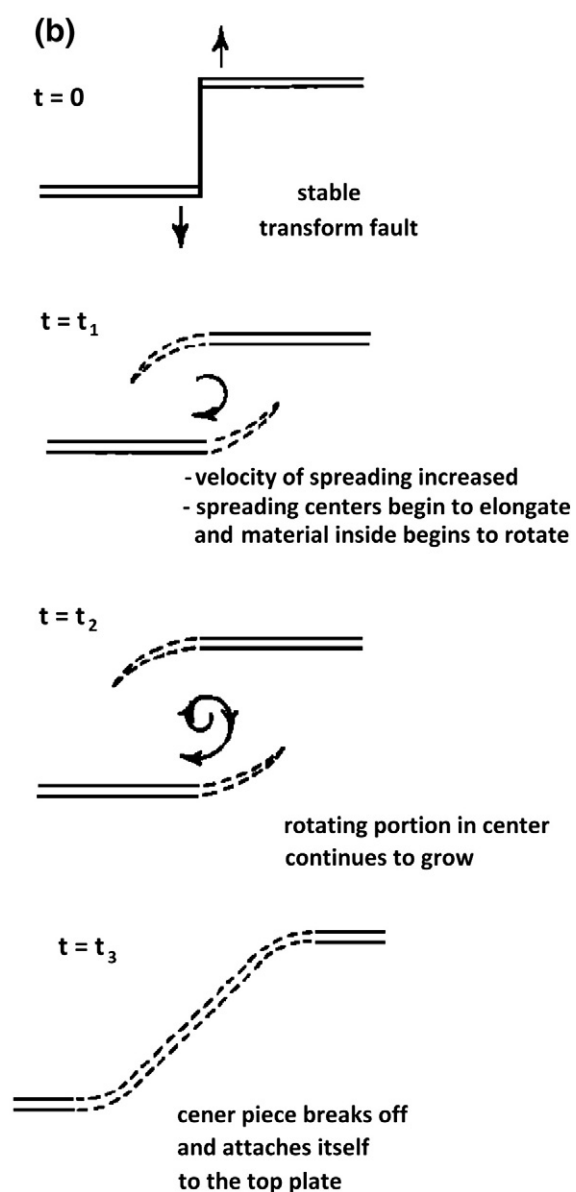


Fig. 2. Dynamics of formation (a) and destruction (b) of transform faults in freezing wax experiments (Oldenburg and Brune, 1975).

spreading centers. The curvature of the initial fractures is probably caused by non-uniformity of the frozen film. The region between the overlapped crests (Fig. 2a) is primarily a zone of shear, and as spreading continues, a crack joining the two spreading centers is generated in this zone. Observation has shown that this may happen in different ways, one of which is depicted in Fig. 2a. The material in the shear zone rotates slightly and is deformed by stretching and folding. A crack is formed parallel to the folds and joins the ends of the spreading centers. This crack is an unstable (oblique) transform fault whose geometry cannot be maintained because ongoing spreading produces compressive forces that change the orientation of the fracture. Consequently, the ridge crests progressively shorten as the transform fault turns towards parallelism with the spreading direction. When this is achieved, no compressive force acts across the transform fault, and neither its orientation nor its length change as spreading continues. An alternative way in which the two spreading centers are often observed to be linked is by a crack generated parallel to the spreading direction. The location of this crack may be anywhere in the overlap zone, but most commonly it is at the end of one of the

spreading centers. This nearly instantaneous development of a stable transform fault is more commonly observed in waxes whose solidified phase has a high tensile strength (Oldenburg and Brune, 1975).

The development of the orthogonal pattern is completed by removing any existing curvature of the spreading centers. Oldenburg and Brune (1972) suggested that thermal effects involving lateral heat conduction in the solid wax were important in straightening out boundary irregularities. They argued that a peninsula of solid wax jutting into the liquid would be expected to accrete material around its periphery more slowly than an indentation in a solidified portion. Although this process may be important in removing small irregularities in the boundary of a ridge crest that is never frozen, a much more efficient method (and one that seems much more applicable to the earth) has been observed. The rates of surface cooling and spreading can be adjusted so that plate separation continues under conditions of alternate freezing and breaking across the ridge crest. The thin film that freezes over the ridge crest is equivalent to the initial zone of weakness in the original breakup except that the newly frozen material appears to be more uniform. Local weaknesses in this zone act as starting points for

ruptures that propagate perpendicular to the spreading direction and thereby quickly and efficiently straighten out irregularities in the original boundary. If the boundary had been very sinuous, the ridge crest might have fractured into two or more spreading ridges joined by transform faults, doing so in a manner already outlined for the main breakup (Oldenburg and Brune, 1975).

Oldenburg and Brune (1972) also documented that transform faults may form at a single straight ridge without overlapping spreading centers. This process was closely associated with an asymmetric spreading documented in some experiments. It was characterized by an irregular ridge axis divided into a number of segments of random length, each spreading asymmetrically in an alternate direction (Fig. 1c). In each segment, the ridge remains stationary with respect to either the moving or fixed plate. In this process, the slow separation allows wax to repeatedly freeze and break across the spreading center. For some unknown reason that Oldenburg and Brune (1972) were not able to elucidate the solidified wax is bound less strongly to one side and, as separation continues, the solid material preferentially breaks away from this side, attaching itself entirely to other plate which therefore grows at a rate equal to the velocity of the moving stick. A schematic example of this evolution of asymmetric spreading is given in Fig. 1c. A type of transform fault that continually increases in length is produced (Oldenburg and Brune, 1972).

Oldenburg and Brune (1975) found that the stability of the orthogonal pattern is dependent on the spreading rate. For certain waxes an orthogonal pattern developed at low spreading velocities disintegrated when the velocity was increased beyond some critical value (Fig. 2b). The pattern disintegration occurred in a variety of ways. Often the corner(s) between the transform fault and the ridge crest would break off. Close examination of these fractured pieces revealed small folds in a direction geometrically consistent with the existence of large resistive forces acting along the transform fault. Deterioration also occurred away from the junctions of the transform fault and spreading centers. In such instances pieces of the solid plate were torn from the transform fault walls and then rotated as they

remained trapped in the zone of shear. In other cases, as the spreading velocity was increased, the resistance to motion along the transform fault appeared to become stronger (see discussion by Oldenburg and Brune, 1975) thus creating larger tensile stresses inside the plates. The ridge crests then began to extend themselves outward in an arcuate manner, and the material in the overlap zone started to rotate (Fig. 2b). The rotating portion (microplate) continued to grow as solid wax accreted to its boundary until eventually the entire portion broke off and attached itself permanently to one of the plates, a curved spreading center being left as end result (Oldenburg and Brune, 1975).

Further details of transform faults origination in freezing wax were reported by O'Bryan et al. (1975). These authors investigated plate accretion when the spreading rate varies along the trench (Fig. 3). Experimental work was based on a combination of Oldenburg and Brune's (1972) wax model and Cox's (1973) tennis ball experiment (Fig. 3a). Various initial cuts were made in a crust formed by cooling on the surface of a pan of molten wax, and portions of the crust were then rotated about a pole of rotation while other portions remained stationary. New thin crust formed in the gap between the rotated portions of the initial crust. The new crust is characterized by a medial spreading center offset by arcuate fractures concentric about the pole of rotation (Fig. 3b). At slow spreading rates (nearer the pole of rotation), the shape of the spreading center is distinctly zigzag, and concentric fractures are lacking. The straight sections of the zigzag possibly originate as shears. At faster spreading rates (farther from the pole of rotation), the zigzag becomes typically orthogonal with straight segments offset by concentric fractures. O'Bryan et al. (1975) proposed, therefore, that the oceanic ridge systems originate as zigzag spreading centers in the asthenosphere or at the base of the lithosphere and then evolve into orthogonal systems that are propagated upward. Like Oldenburg and Brune (1972), O'Bryan et al. (1975) observed straightening of irregular and curved spreading boundaries due to differential cooling and accretion. This process caused the zigzag spreading center to evolve into straight spreading-center segments separated by arcuate fractures (Fig. 3c) (O'Bryan et al., 1975). These observations

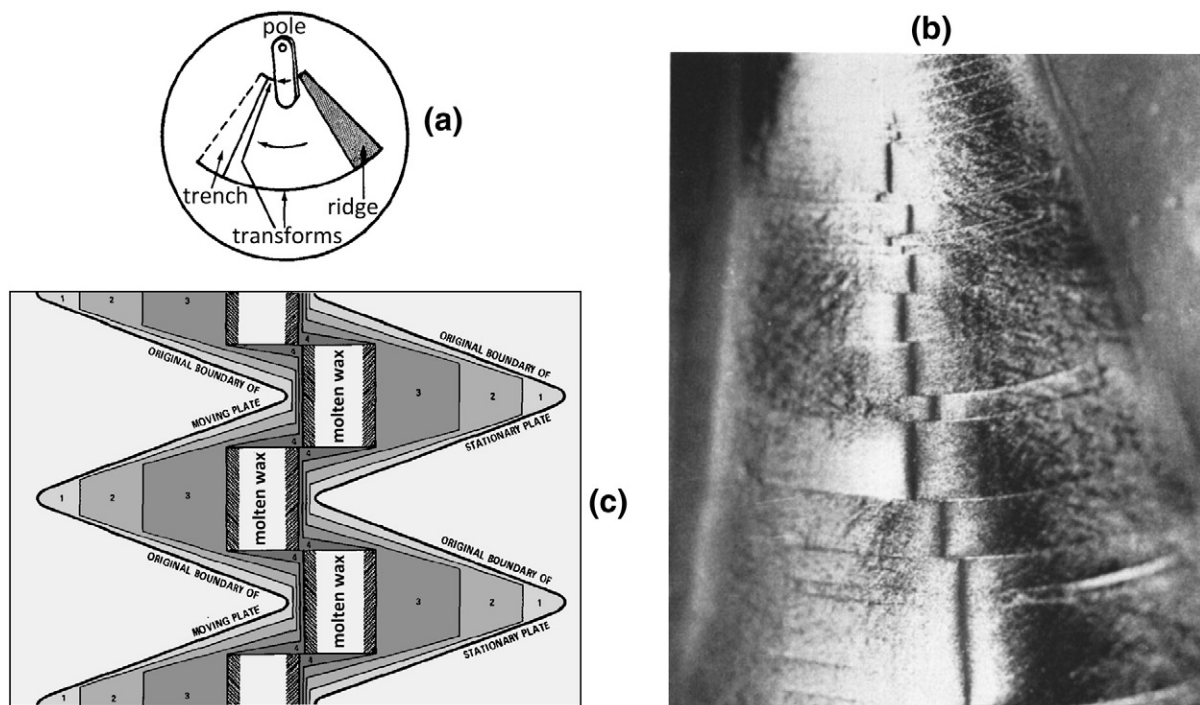


Fig. 3. Freezing wax experiment of O'Bryan et al. (1975): (a) model setup, (b) typical experimental result, (c) schematic representation of asymmetric/differential plate accretion and cooling in case of nucleation of orthogonal spreading centers and transform faults from initial zigzag spreading pattern.

further suggest that the orthogonal pattern in freezing wax experiments is not an instantaneous result of plate fragmentation. Instead, formation of this pattern is a gradual process associated with long-term plate separation, cooling and accretion.

Later, several more analog studies were conducted with freezing wax (Katz et al., 2005; Ragnarsson et al., 1996). None of these studies reproduced the orthogonal ridge-transform fault pattern successfully modeled by Oldenburg and Brune (1972) and O'Bryan et al. (1975). Most likely this was caused by modified physical/chemical properties and microstructures (e.g., Freund and Merzer, 1976) of waxes used in these later experiments. In particular, Ragnarsson et al. (1996) reported results on the rift formation between two freezing wax plates floating on molten wax which are pulled apart at a constant velocity. Motivated by the prior experimental investigations of Oldenburg and Brune (1972), Ragnarsson et al. (1996) also used Shellwax 120 in their experiments but obtained different results. Several distinct patterns were observed for larger spreading rates; a stable straight rift, a spiky rift with fracture zones almost (but not exactly) parallel to the spreading direction, and a regular zigzag pattern characterized by an angle dependent on the spreading rate. The characteristic angles of the zigzag pattern agree with a simple geometrical model. Coarsening of the pattern over time, the three-

dimensional structure and the topography of the crust were also investigated (Ragnarsson et al., 1996).

Katz et al. (2005) utilized Shell Callista 158 wax for investigating spontaneous formation of tectonic microplates (e.g., Fig. 2b) – the extension mode that is alternative to the orthogonal ridge-transform fault pattern at higher spreading rate (Oldenburg and Brune, 1975). Rotating, growing microplates were observed in a wax analog model of sea-floor spreading. Paired, relatively short and poorly pronounced transform faults often formed at two margins of the microplates. It was found that wax microplates are kinematically similar to sea-floor tectonic microplates in terms of spreading rate and growth rate. Furthermore, their spiral pseudo-fault geometry is quantitatively consistent with oceanic microplate growth model proposed by Schouten et al. (1993). This model states that the rigid motion of a microplate is like that of a ball rotating between two parallel, moving plates. Unlike the ball, however, a microplate grows by accreting young lithosphere. Like oceanic microplates (Hey et al., 1995), wax microplates originate from overlapping spreading centers which nucleate frequently on the spreading rift. Nucleation of wax overlapping spreading centers occurs predominantly on sections of obliquely spreading rift, where the rift normal is about 45° from the

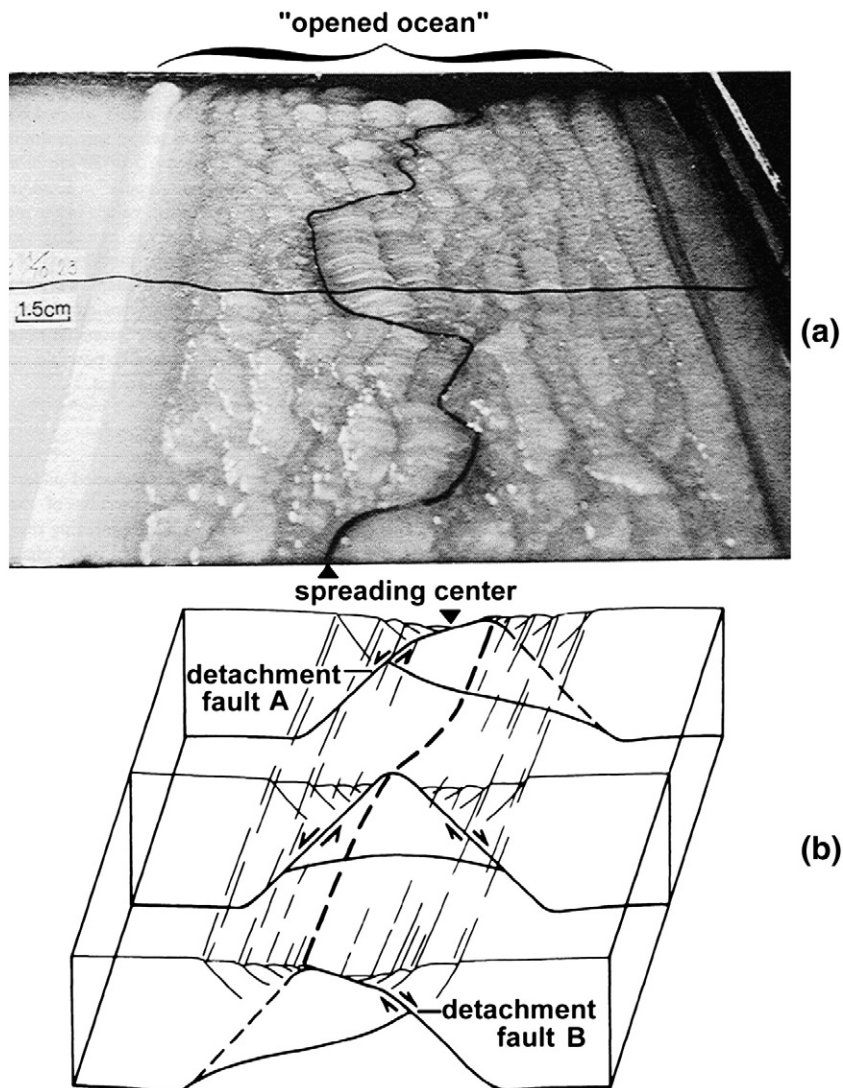


Fig. 4. Thermomechanical model of slow spreading by Shemenda and Grocholsky (1994): (a) model with strongly curved ridge, (b) schematic representation of transfer zone accommodating change in the polarity of spreading asymmetry to the opposite; two detachment faults (A and B) control the asymmetry.

spreading direction. The diminished divergence component across these segments allows the rift axis to freeze, introducing a discontinuity in the rift and a local stress field that tends to cause propagation of the rift tips into an overlapping geometry (De Bremaecker and Swenson, 1990; Sempere and Macdonald, 1986). This process is opposite to the destruction of the transform fault (Fig. 2b) (Oldenburg and Brune, 1975). The rift tips will propagate in this manner only if the tensile strength of the adjacent lithosphere is small compared to that of the frozen rift. If, on the other hand, the adjacent lithosphere is too strong to be fractured by rift-tip propagation, deformation and faulting will remain in the rift center. A muted strength contrast might be expected at fast spreading ridges where the adjacent lithosphere is thinner and weaker than at slow spreading ridges, consistent with the distribution of microplates on Earth (Katz et al., 2005).

Further insightful analog experiments were conducted by Shemenda and Grocholsky (1994) with the use of an alloy of solid hydrocarbons (paraffins and ceresines) and mineral oils. A properly scaled thermo-mechanical experimental model of slow seafloor spreading is developed to investigate the mechanism of lithosphere accretion (Fig. 4). The crystallizing upper layer (the lithosphere) possesses semiplastic-semibrittle properties. Spreading in the model is very unstable, asymmetric, and involves regular jumps of the spreading center. While the ridges can be strongly curved (Fig. 4a) the transform faults are not well pronounced. In contrast, detachment faults are very common and often control deformation at the plate boundary resulting in the asymmetric plate accretion (Fig. 4b). Scaling up the experimental results to match seafloor spreading yielded the length of the jumps of about 10 km and the period of the order of 10^5 – 10^6 years. Similarly to nature, the dimensions of the valley, as well as the overall seafloor relief, are strongly dependent on the spreading rate: the lower the value, the rougher the relief. The jumps of the spreading centers are not synchronous along the plate boundary. Moreover, they can be of different types, with varying distances and in opposite directions on adjacent segments of the spreading axis, leading to the occurrence of transfer or accommodation zones (Shemenda and Grocholsky, 1994).

3.2. Non-accreting analog models

Significant analog modeling efforts were directed toward understanding of internal structures and surface expressions of oceanic transform faults and oblique rifting processes (e.g., Dauteuil et al., 2002; Dauteuil and Brun, 1993; Mauduit and Dauteuil, 1996). In the systematic study of Dauteuil et al. (2002) the models are made of sand and silicone putty as analogs of the brittle and viscous layers of the lithosphere, respectively. Two plastic sheets coming from shifted gashes form a setup of two diverging discontinuities connected by a transform boundary (Fig. 5a). The rheological layering and strength of the model were modified using different shapes of the viscous layer placed on the transform boundary. Above the divergent discontinuities, the faulting pattern is always formed by parallel normal faults (Fig. 5b, c). When no viscous layer is placed on the transform boundary (strong discontinuity), the deformed zone is narrow and has few linear faults (Fig. 5, model FT-1). By adding a narrow and thin viscous layer, the deformed zone becomes wider with a complex faulting pattern formed by oblique-slip faults on the limits of this zone and by pure strike-slip faults in its inner part (Fig. 5, model FT-2). These pure strike-slip faults are oblique to the transform boundary. When a large viscous layer covers the weak transform discontinuity, faulting is dominated by widely distributed normal faults and strike-slip faults are restricted to the inner part of the deformed zone (Fig. 5, model FT-3). Dauteuil et al. (2002) applied these results to 24 oceanic transform zones and concluded that the spreading rate and the transform offset are the two dominant parameters controlling the lithospheric strength at the transform boundary, and thus the deformation pattern.

Marques et al. (2007) used scaled physical modeling to investigate spontaneous fracturing in an oceanic lithosphere overlying a less dense asthenosphere. In the models, an upper wedge-shaped layer of sand represented an oceanic lithosphere; a lower layer of polydimethylsiloxane (PDMS), mixed with dense wolframite powder, represented the asthenosphere (Fig. 6a). In the models, as in nature, isostatic compensation resulted in uplift of ridges and subsidence on their flanks. The resulting relief was responsible for ridge push. The style of normal faults in the axial rift zone depended on the local thickness of the brittle sand layer (Fig. 6b and c). In a model with thin lithosphere at the ridge crest and no embedded weakness in the fault, ridge push was responsible for a short transform fault, linking en-echelon rifts (Fig. 6b). In a similar model, but with thick lithosphere, an oblique rift formed at about 20° to the offset trace (Fig. 6c). Marques et al. (2007) concluded that ridge push was not adequate to create an ideal transform fault. In a model of an offset ridge, with an embedded thin vertical layer of pure PDMS at 90° to the ridge, transform motion concentrated along this weak layer, and the resulting structural style was very similar to that in nature (Fig. 6d). On the basis of these results, Marques et al. (2007) inferred that, in nature, ridge push can drive strike-slip motion on transform faults, provided that these are weaker than the adjacent oceanic lithosphere and that they form early in the history of spreading.

Tentler (2003a, 2003b, 2007) and Tentler and Acocella (2010) performed analog studies to investigate how the initial configuration of initially offset oceanic ridge segments affect nucleation of transform faults and overlapping spreading centers. The centrifuge models (Fig. 7a) of Tentler and Acocella (2010) consist of a lighter silicone, rising within a denser silicone below a brittle layer simulating the oceanic lithosphere and composed of a mixture of Vaseline (60%), paraffin (20%) and gypsum powder (20%). Precut fractures in the brittle layer simulated the initial configuration of oceanic ridges. The rise and lateral spreading of the lighter silicone induce the propagation, widening, interaction, and linkage of the lithospheric fractures (Fig. 7b–c). Tentler and Acocella (2010) varied the offset and overlap between the precut fractures, obtaining several distinctive types of interaction between the ridge segments (Fig. 7d). Increase of fracture overlap leads to interaction zones of lower aspect ratio, with fractures propagating at lower angles to the mean extension direction. Increase of offset leads to the elongation of the interaction zones with the new fractures propagating subparallel to the extension direction. The authors compared analog models with several examples of natural ridges and identified close geometric similarities, confirming the existence of predominant types of ridge interaction. Among these, ridges with smaller offsets develop interactions similar to overlapping spreading centers, whereas ridges with larger offsets have geometries reminiscent of transform zones. Based on the comparison between experimental and natural examples Tentler and Acocella (2010) suggested that the wide spectrum of ridge interaction types in nature results from the initial configuration of the divergent plate boundary.

It should be mentioned that in contrast to freezing wax models (e.g., Katz et al., 2005; O'Bryan et al., 1975; Oldenburg and Brune, 1972; Shemenda and Grocholsky, 1994), analog modeling approaches involving brittle lithosphere (e.g., Dauteuil et al., 2002; Dauteuil and Brun, 1993; Marques et al., 2007; Mauduit and Dauteuil, 1996; Tentler, 2003a, 2003b, 2007; Tentler and Acocella, 2010) do not permit accretion of the upper brittle lithospheric layer. Consequently, results of these models are rather applicable for understanding the nucleation of various plate fragmentation patterns during initial stages of spreading. These results are, however, less suitable for explaining ridge-transform fault patterns formed during long-term plate separation and accretion (e.g. O'Bryan et al., 1975; Oldenburg and Brune, 1972). On the other hand, freezing wax experiments often produced open spreading centers (e.g., Fig. 3b) where liquid wax was exposed to the surface (e.g., O'Bryan et al., 1975; Ragnarsson et al.,

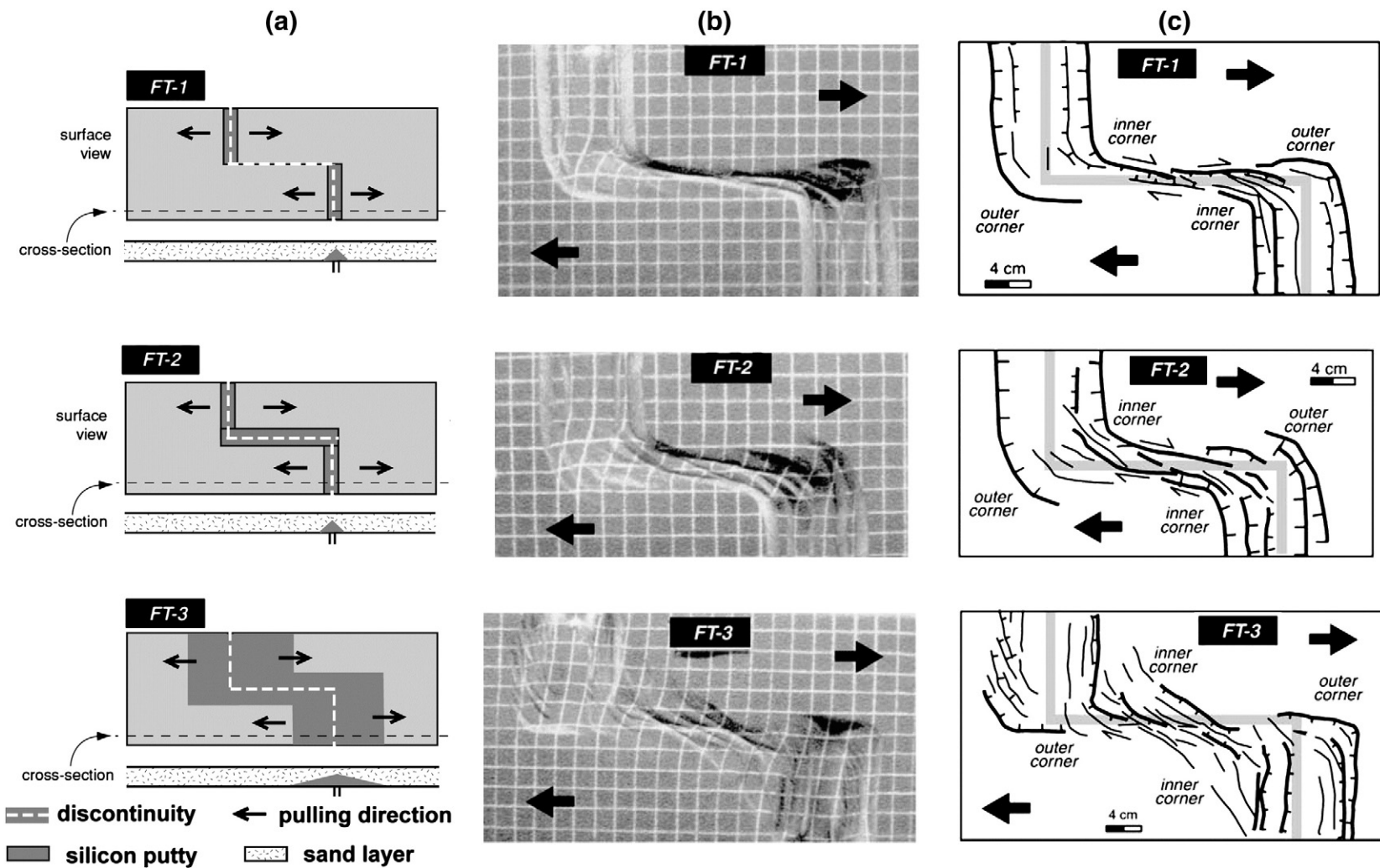


Fig. 5. Analog model with non-accreting brittle lithosphere by [Dauteuil et al. \(2002\)](#). (a) Tested model setups: FT-1 without a silicone band on the transform discontinuity; FT-2 with a narrow silicone band on the transform discontinuity; FT-3 with a wide silicone band. (b), (c) Experimental results: (b) surface photographs of the experiments at the end of the deformation; (c) sketch drawings of fault patterns. The light gray line in (c) indicates initial location of diverging and transfer discontinuities.

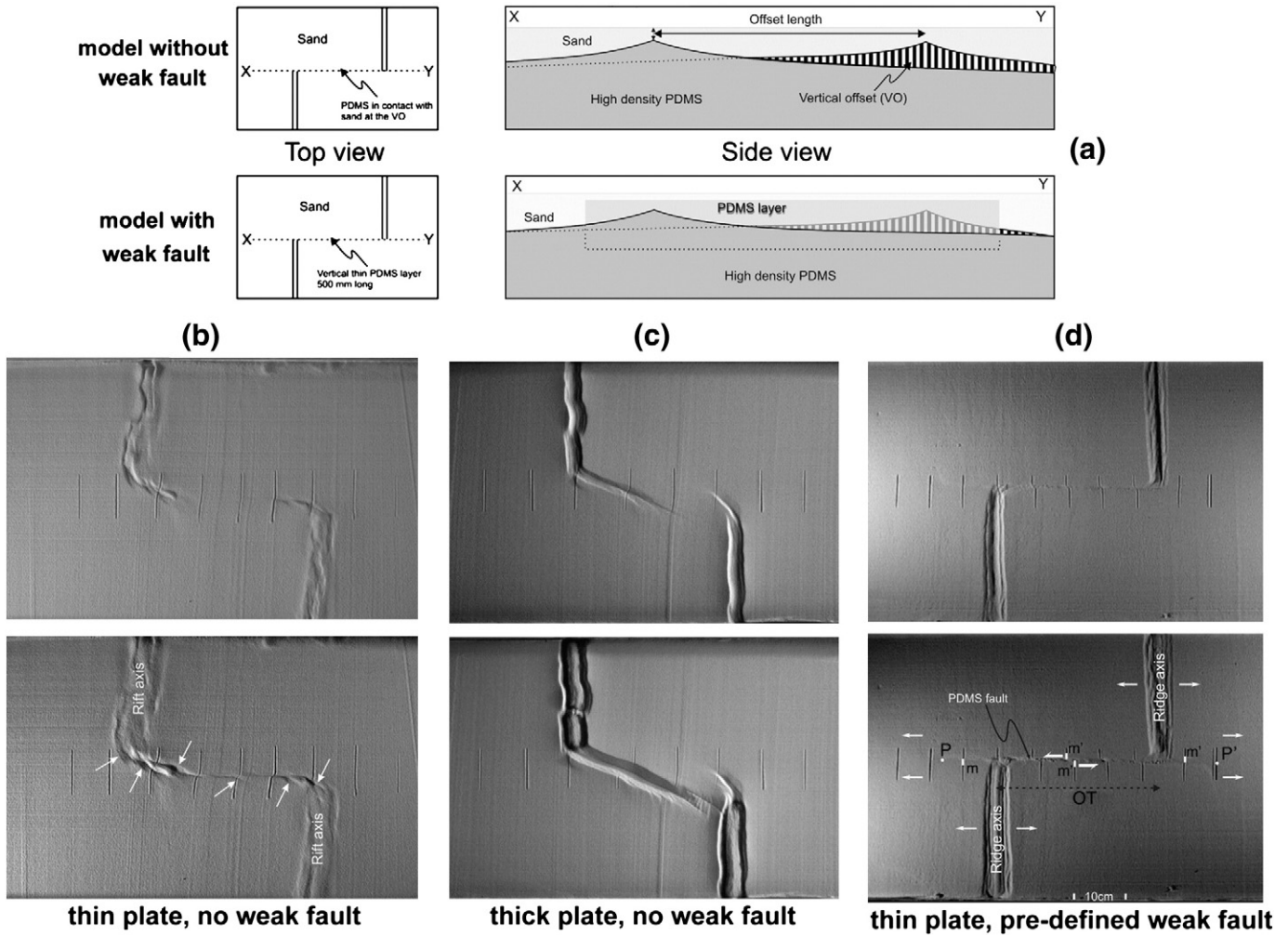


Fig. 6. Analog model with non-accreting brittle lithosphere by Marques et al. (2007). (a) Tested model setups. (b)–(d) Experimental results: (b) thin lithosphere at ridge axes, no embedded fault, (c) thick lithosphere at ridge axes, no embedded fault, (d) thin lithosphere at ridge axes, embedded weak fault.

1996). This is obviously dissimilar to nature where mantle-derived magmas mostly crystallize at depth and spreading centers are always covered by the solid oceanic crust.

4. Numerical modeling of transform faults

Numerical modeling of transform faults started in the late 1970s and includes both mechanical and thermomechanical approaches. Three main types of model setups were investigated numerically: models of stress and displacement distribution around transforms, models of their thermal structure and crustal growth, and models of nucleation and evolution of ridge-transform fault patterns.

4.1. Models of stress and displacement distribution

Earliest numerical models of transform faults were often addressing deformation and stress distribution around these oceanic floor structures (e.g., Behn et al., 2002; Fujita and Sleep, 1978; Gudmundsson, 1995; Hashima et al., 2008; Phipps Morgan and Parmentier, 1984).

Fujita and Sleep (1978) conducted a remarkable numerical study by using a 2D anisotropic, two-dimensional finite element model to determine constraints on relative material properties and the horizontal stress field of mid-ocean ridges near transform faults given the regional stress field. Various ridge geometries including one and two transforms were analyzed numerically. The following

conclusions were made on the basis of this study (Fujita and Sleep, 1978):

- A ratio of 1000 in the viscous equivalent of Young's modulus between the ridge crest and the oceanic plate was indicated.
- The horizontal stress field suggests that the concentration of near ridge-transform intersection seamount chains and the occurrence of ridge jumps are a result of regional stresses. Since dikes are perpendicular to local deviatoric tension, ridges are shown to become oblique such that the connecting transform fault is shortened.
- Excessively oblique ridges, however, tend to produce intrusions that cancel that obliqueness. There is, however, a preference towards the development of oblique ridge segments for slow spreading ridges.
- Thermal variations related to hot spots are unlikely to cause asymmetric spreading.
- Overshooting by long ridge segments will preempt short ridge segments and cause lineaments on the sea-floor.

Later work of Phipps Morgan and Parmentier (1984) investigated stress distribution near a ridge-transform intersection with the use of 2D finite element model with prescribed plate boundary stresses. This study was aimed to understand distribution of plate boundary stresses based on natural observation that the spreading axis and the normal fault scarps, which parallel the ridge axis away from the intersection, locally curve toward the transform fault. This observation implies that the least compressive stress direction becomes oblique to the spreading direction near the ridge-transform intersection.

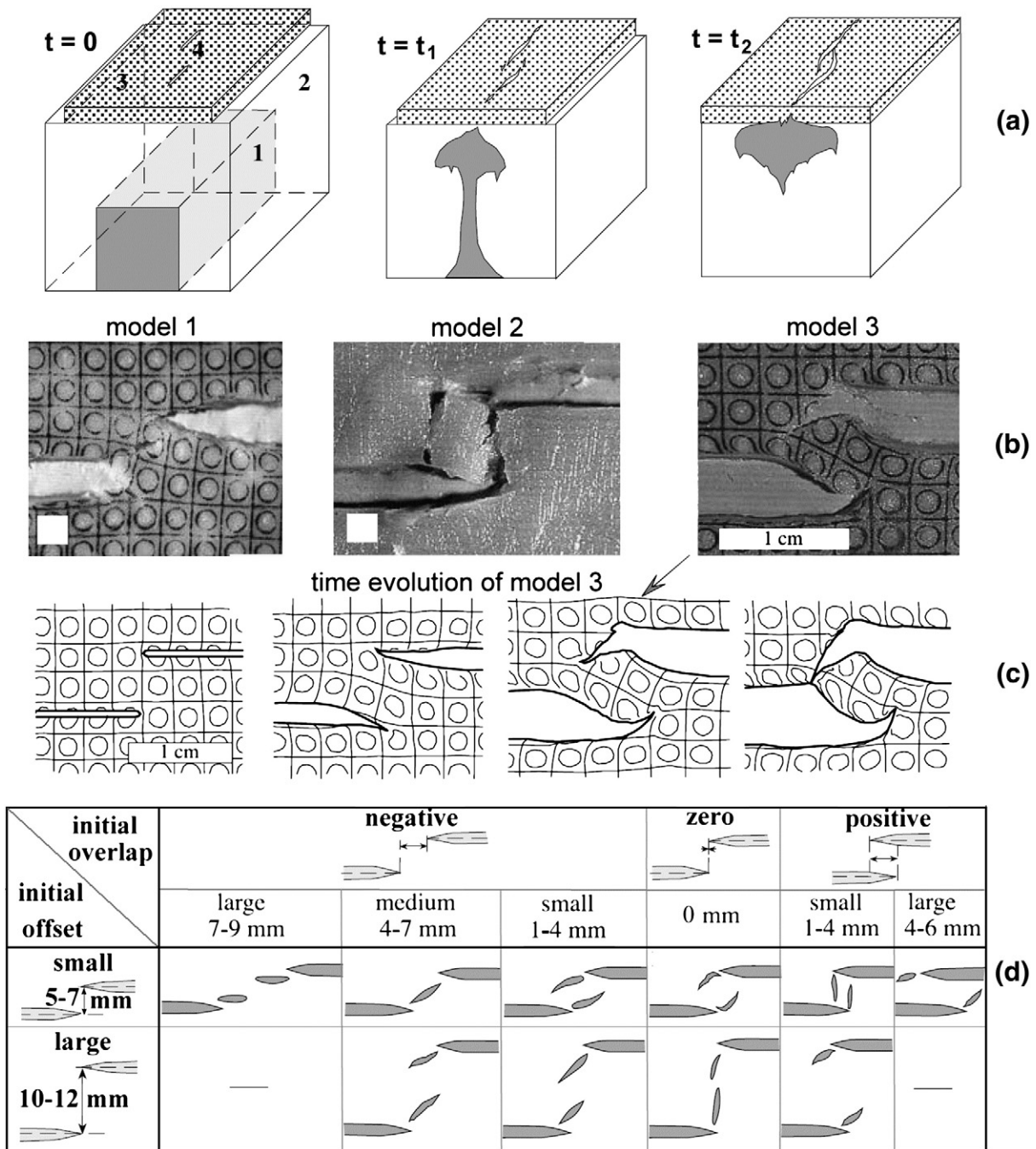


Fig. 7. Centrifuge model with non-accreting brittle lithosphere by [Tentler and Acocella \(2010\)](#). (a) Experimental setup: (1) lower-density silicone, simulating the asthenosphere; (2) higher-density silicone, simulating the upper mantle; (3) the uppermost brittle layer, simulating the oceanic lithosphere; and (4) pre-cut fractures. (b) Examples of different types of fracture interactions in a map view. (c) Evolution of the reference model 3. (d) Types of interaction between two pre-cut parallel fractures in the brittle layer of models.

Modeling results suggested that the orientation of the least compressive stresses strongly depends on the stresses applied at plate boundaries. Thus, faulting patterns observed near transforms can be used to constrain distribution of plate boundary forces acting in different mid-ocean ridges ([Phipps Morgan and Parmentier, 1984](#)).

[Gudmundsson \(1995\)](#) conducted a numerical boundary element study aimed to understand stresses acting inside oceanic transform faults. Although their formation is commonly attributed to shear stresses, these faults contain many structural elements indicating extension across them. Examples include transform-parallel tension fractures, normal faults, grabens, dykes and small-scale spreading centers ([Gudmundsson, 1995](#) and references therein). The results of Gudmundsson's modeling (1995) showed that uniaxial tensile

loading (plate pull) parallel with the transform fault tends to lock it but also gives rise to shear-stress concentration in a zone that coincides with the fault. This shear stress is primarily responsible for strike-slip faulting and associated earthquakes in the transform fault. To generate the transform-parallel fracture-zone graben, normal faults, tensile fractures, dykes and spreading centers, however, requires tensile loading parallel with the ridge axis. The results suggested that biaxial (ridge-parallel and ridge-perpendicular) tensile loading generates a stress field that: (i) unlocks and makes slip easier on the transform faults; (ii) and explains the oblique fractures at the ridge-transform junctions ([Gudmundsson, 1995](#)).

Problem of asymmetry of faulting pattern and topography at ridge-transform intersections was further investigated by [Behn et al. \(2002\)](#)

with a 3D mechanical boundary element model. Near the intersection, axial topography is consistently asymmetric, with crust on the inside-corner elevated relative to that on the outside-corner (e.g., Karson and Dick, 1983). Similar asymmetry is also reflected in the pattern of seafloor faulting and abyssal hill fabric. In particular, faults extending from the segment center into inside-corner crust curve sharply in the offset direction, while faults extending into outside-corner crust typically remain parallel to the ridge. Behn et al. (2002) conducted a series of numerical experiments to investigate the effects of oceanic transform faults on stress state and fault development at adjacent mid-ocean ridge spreading centers. An elastic plate with uniform thickness and an upper free surface was used in this model. The model geometry includes two kinematically prescribed, vertical, uniformly opening spreading centers offset by a prescribed orthogonal transform fault. In accordance with the results of analog models (e.g., Oldenburg and Brune, 1972, 1975) Behn et al. (2002) found that the time-averaged strength of transform faults is low, and that transform faults behave as zones of significant weakness on time scales longer than a typical earthquake cycle. Specifically, mechanical coupling of only ~5% best explains the observed patterns of strike-slip and oblique normal faulting near a ridge-transform intersection. On time scales shorter than a typical earthquake cycle, transient “locked” periods can produce anomalous reverse faulting similar to that observed at the inside corner of several slow-spreading ridge segments. Behn et al. (2002) also predicted that ridge-normal extension will be somewhat suppressed at the inside corner due to the shear resistance along the weak transform. This implies that an alternative mechanism is necessary to explain the preferential normal fault growth and enhanced microseismicity observed at many inside corners (Behn et al., 2002).

Recently, Hashima et al. (2008) conducted analytical–numerical study in the framework of elasticity theory and demonstrated its applicability for the deformation around transform faults during the repetitive earthquake cycles that are common in nature (e.g., Reichle et al., 1976). The authors succeeded in obtaining general expressions for internal deformation due to a moment tensor in an elastic/viscoelastic multilayered half-space under gravity. As one of numerical examples Hashima et al. (2008) considered the deformation cycles associated with the periodic occurrence of interplate strike-slip earthquakes in the ridge-transform fault system. In the computed 2D numerical model the ridge-transform fault system divides the 10-km-thick elastic surface layer overlying a viscoelastic substratum into two plates. The authors assumed steady opening of spreading centers and periodic stick-slip motions at the transform fault with intervals of 100 yr. The model allowed computing the temporal change of the horizontal displacement field at the plate surface during one earthquake cycle. It was demonstrated that the occurrence of a strike-slip earthquake at the transform fault completely releases the distortion of the horizontal displacement field produced by the opening of the spreading centers in the interseismic period (Hashima et al., 2008).

4.2. Models of thermal structure and crustal growth

Another important, early direction in computational modeling was aimed to understand the thermal structure and crustal growth of transform faults (e.g., Forsyth and Wilson, 1984; Furlong et al., 2001; Phipps Morgan and Forsyth, 1988; Shen and Forsyth, 1992). In particular, Phipps Morgan and Forsyth (1988) combined a semi-analytical solution for uniform viscosity mantle flow with 3D numerical solution for temperature field based on finite differences. This model is applied to study an idealized spreading center consisting of a 100 km transform fault offsetting two ridge segments spreading at rates of 10, 20, and 40 mm/yr (half rates). Using an adiabatic melt relation together with the flow and temperature calculations, the authors found the distribution of melt production beneath the spreading center. Finally, an analytical porous flow model of melt migration within a spreading center was used to assess the possible effects of melt migration on oceanic crustal structure. Phipps Morgan

and Forsyth (1988) found that the topographic effects caused by variations of mantle density associated with cooling near a transform offset are much smaller than the observed 1 km seafloor deepening within 30 km of a fracture zone. It was suggested that variations of crustal thickness can explain (as one of the possible candidate mechanisms) this seafloor deepening and that several kilometers of crustal thinning can plausibly occur within 30 km of a fracture zone. This thinning is due to both perturbations in melt migration at a transform offset with melt preferentially migrating toward the center of a spreading segment and perturbations in melt production near a transform offset caused by lower upwelling rates near the transform. The major influence of a transform offset on melting beneath a ridge-transform spreading center is due to the muting effect of the transform offset on upwelling beneath the ridge-transform intersection; lower rates of upwelling lead to lower amounts of melt production within a broad region near the transform (Phipps Morgan and Forsyth, 1988).

Later, Shen and Forsyth (1992) investigated similar idealized ridge-transform setup with a fully coupled 3D thermomechanical numerical model combining a finite element method to solve for the three-dimensional flow and a finite difference solution for temperatures. More realistic temperature dependent Newtonian and non-Newtonian (power law) mantle rheologies were tested. It was demonstrated that mantle upwelling in the variable-viscosity model is stronger but narrower compared to isoviscous models. Faster upwelling reduces heat loss to the surface during ascent, leading to greater melt production. Consequently, the variable-viscosity model creates thicker crust and the predicted thickness is more nearly independent of spreading rate. The zone of melt production is narrower and the rate of melt production decreases more abruptly near the transform fault (Shen and Forsyth, 1992).

Behn et al. (2007) used 3D finite element simulations to investigate the temperature structure beneath oceanic transform faults in case of non-Newtonian mantle rheology that incorporates brittle weakening of the lithosphere. In contrast to simpler rheological models (e.g., Furlong et al., 2001; Phipps Morgan and Forsyth, 1988; Shen and Forsyth, 1992), experiments of Behn et al. (2007) generated a region of enhanced mantle upwelling and elevated temperatures along the transform; the warmest temperatures and thinnest lithosphere are predicted to be near the center of the transform. The authors showed that this warmer temperature structure is consistent with a wide range of observations from ridge-transform environments, including the depth of seismicity, geochemical anomalies along adjacent ridge segments, and the tendency for long transforms to break into small intra-transform spreading centers during changes in plate motion (Behn et al., 2007).

Two years later, Gregg et al. (2009) published results from a combined 3D petrological–thermomechanical numerical study (Fig. 8) aimed to understand thermal structure and crustal growth processes in fast slipping transform faults (e.g. Gregg et al., 2007 and references therein). The authors examined mantle melting, fractional crystallization, and melt extraction beneath fast slipping, segmented oceanic transform fault systems. The 3-D mantle flow field and temperature are calculated using the finite element method for the model with the non-deforming upper boundary (Fig. 8a). Mantle flow is driven by the movement of two surface plates diverging at a half-spreading rate. Sectioned mid-ocean ridge with a single segmented transform fault is defined by the kinematic boundary condition imposed on the top of the model. Three-dimensional mantle flow and thermal structures are calculated using a temperature-dependent rheology that incorporates a viscoplastic approximation for brittle deformation in the lithosphere. Thermomechanical solutions are combined with the melting model of Kinzler and Grove (1992a, 1992b, 1993) to determine 3D geometry of melting zone (Fig. 8b) and major element melt composition. Gregg et al. (2009) investigated the mantle source region of intra-transform spreading centers using the melt migration approach of Sparks and Parmentier (1991) for two end-member pooling models (Fig. 8b): (1)

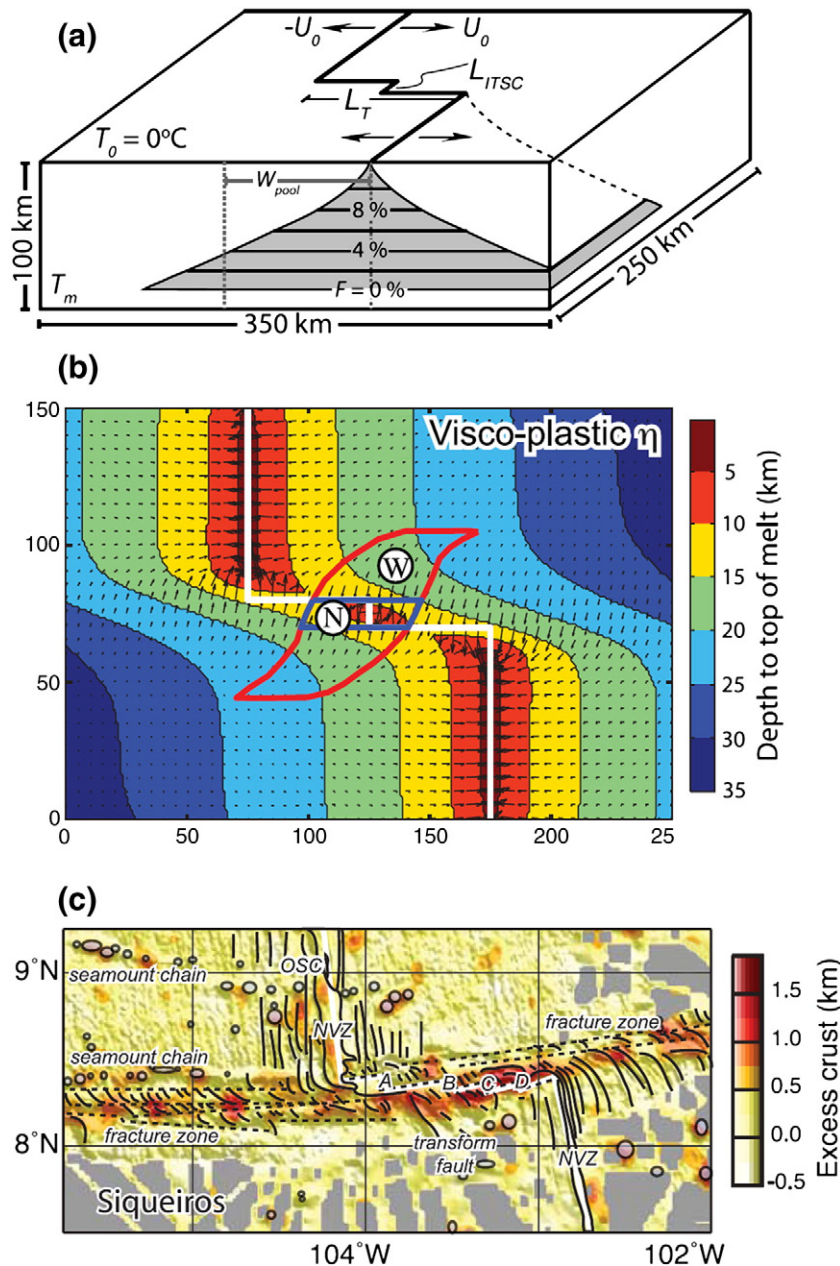


Fig. 8. 3D numerical modeling experiments of [Gregg et al. \(2009\)](#). (a) Model setup. (b) Calculated depth to the top of the melting region. Regions W (red outline) and N (blue outline) delineate the wide and the narrow melt pooling models, respectively. (c) Natural example of lateral variations in crustal thickness in transform fault derived from residual mantle Bouguer gravity calculations ([Gregg et al., 2007](#)). Excess crust is defined as the deviation for the reference crustal thickness of 6 km.

a wide pooling region that incorporates all of the melt focused to the intra-transform spreading center and (2) a narrow pooling region that assumes melt will not migrate across a transform fault or fracture zone. The model with wide melt pooling can explain both the systematic crustal thickness excesses observed at intermediate and fast slipping transform faults (e.g. [Gregg et al., 2007](#)) as well as the deeper and lower extents of melting observed in the vicinity of several transform systems. Applying these techniques to the Siqueiros transform on the East Pacific Rise [Gregg et al. \(2009\)](#) found that both the viscoplastic rheology and wide melt pooling are required to explain the observed variations in gravity inferred crustal thickness ([Fig. 8c](#)). It was also shown that mantle potential temperature of 1350 °C and fractional crystallization at depths of 9–15.5 km fit the majority of the major element geochemical data from the Siqueiros transform fault system ([Gregg et al., 2009](#)).

4.3. Models of nucleation and evolution

[Stoddard and Stein \(1988\)](#) presented very particular 2D kinematic model of an orthogonal ridge-transform faults system subjected to an asymmetric accretion. The main idea behind this relatively simple kinematic model is that spreading ridge-transform geometries will remain stable only in case of ideally symmetric accretion. Asymmetric accretion, however, will cause lengthening or shortening of transforms and, in extreme cases, may result in zero-offset transforms (zero offset fracture zones) (e.g., [Shouten and White, 1980](#)) and very-long-offset transforms such as the Ninetyeast and Chagos transforms ([Stoddard and Stein, 1988](#)). [Stoddard and Stein \(1988\)](#) examined the effects of various parameters on the evolution of zero-offset transforms and very-long-offset transforms. Starting with the transform

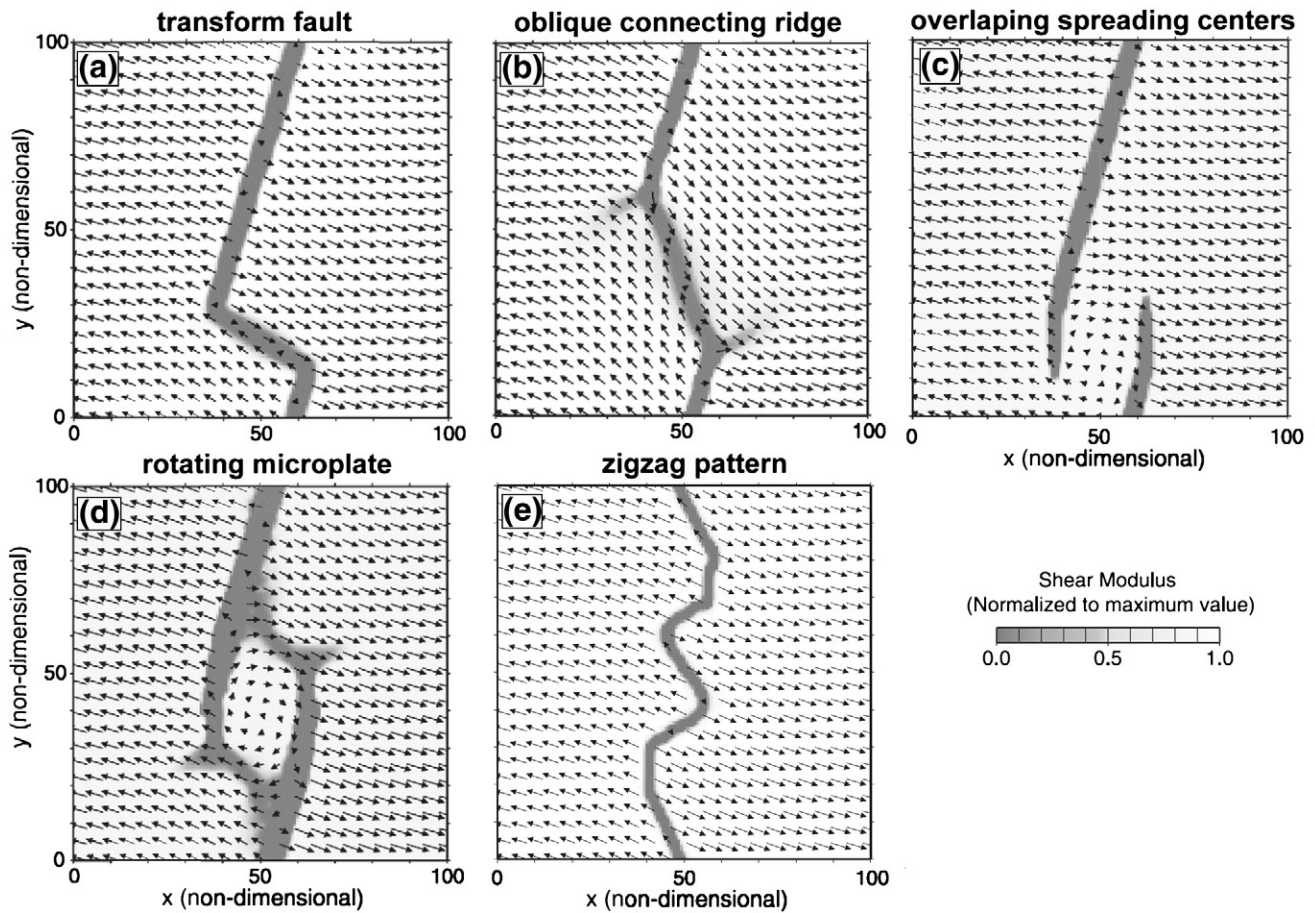


Fig. 9. Results of numerical experiments of Hieronymus (2004) showing fundamental modes of plate fragmentation with pre-defined ridge offset: (a) transform faults, (b) oblique connecting spreading centers, (c) overlapping spreading centers, (d) microplates, and (e) zigzag ridges.

length spectrum found along the Mid-Atlantic Ridge distributed in a randomly determined ridge-transform configuration, the authors allowed for asymmetric accretion along ridge segments, assuming that individual ridge segments act independently. Results of the experiments were analyzed for the effects of initial configuration, degree of asymmetry, and degree of bias in asymmetry on the generation of very-long offset and zero-offset transforms. This model predicts that zero-offset transforms can be actually generated with a minimum degree of accretion asymmetry, and that bias in the asymmetry and initial ridge-transform-ridge configuration has no effect on generation of these structures. On the other hand, random variations in spreading asymmetry have difficulty generating significant increases in transform length. Consequently, very-long-offset transforms should rather be manifestations of specific dynamic processes operating at respective mid-ocean ridges (Stoddard and Stein, 1988).

Most recently numerical modeling of transform faults turned toward addressing processes of their spontaneous nucleation. Hieronymus (2004) performed 2D mechanical study of control on seafloor spreading geometries by stress- and strain-induced lithospheric weakening that was inspired by variability of natural spreading patterns such as orthogonal ridge-transform fault patterns, overlapping spreading centers and microplates. In order to understand this variability Hieronymus (2004) developed a dynamical 2D model of spreading using two independent, scalar types of damage in an extending elastic plate. The simple elastic damage model introduced by Hieronymus (2004) displays most of the failure modes exhibited by the oceanic lithosphere and by analog wax models (e.g., O'Bryan et al., 1975; Oldenburg and Brune, 1972, 1975).

Given an initial distribution of imperfections defining ridge offset, the system is able to self-organize into a ridge-transform pattern in which divergent and shear deformation are localized into separate zones. The following important predictions were made on the basis of this model (Hieronymus, 2004):

- It is possible to generate the transform-ridge geometry as well as other observed spreading configurations (Fig. 9) with a relatively simple elastic plate model. Coupling to the viscous mantle is not required, and the observed prominence of melt generation at the center of ridge segments relative to the segment ends (Bonatti, 1996) may thus be the result rather than the cause of ridge segmentation.
- Only a small number of spreading geometries are dynamically possible in the model (Fig. 9). These are transform faults, microplates, overlapping spreading centers, zigzag ridges, and oblique connecting ridges at 45° relative to the principal stresses, all of which are observed along MORs.
- Transform faults form by gradual focusing of initially diffuse damage requiring a stress-dependent rheology.
- The condition that transform faults be weaker than the pristine plate (Oldenburg and Brune, 1975) is necessary for transform stability but not sufficient for transform formation. The rate of shear damage formation relative to that of ridge propagation is the main factor controlling the formation of transform faults.
- Microplates are a fundamental mode of oceanic spreading. Changes in plate motion are not required (e.g., Engeln et al., 1988), although they may help in destabilizing the orthogonal spreading pattern.
- Stable overlapping spreading centers require material properties different from those for microplates. The fact that overlapping

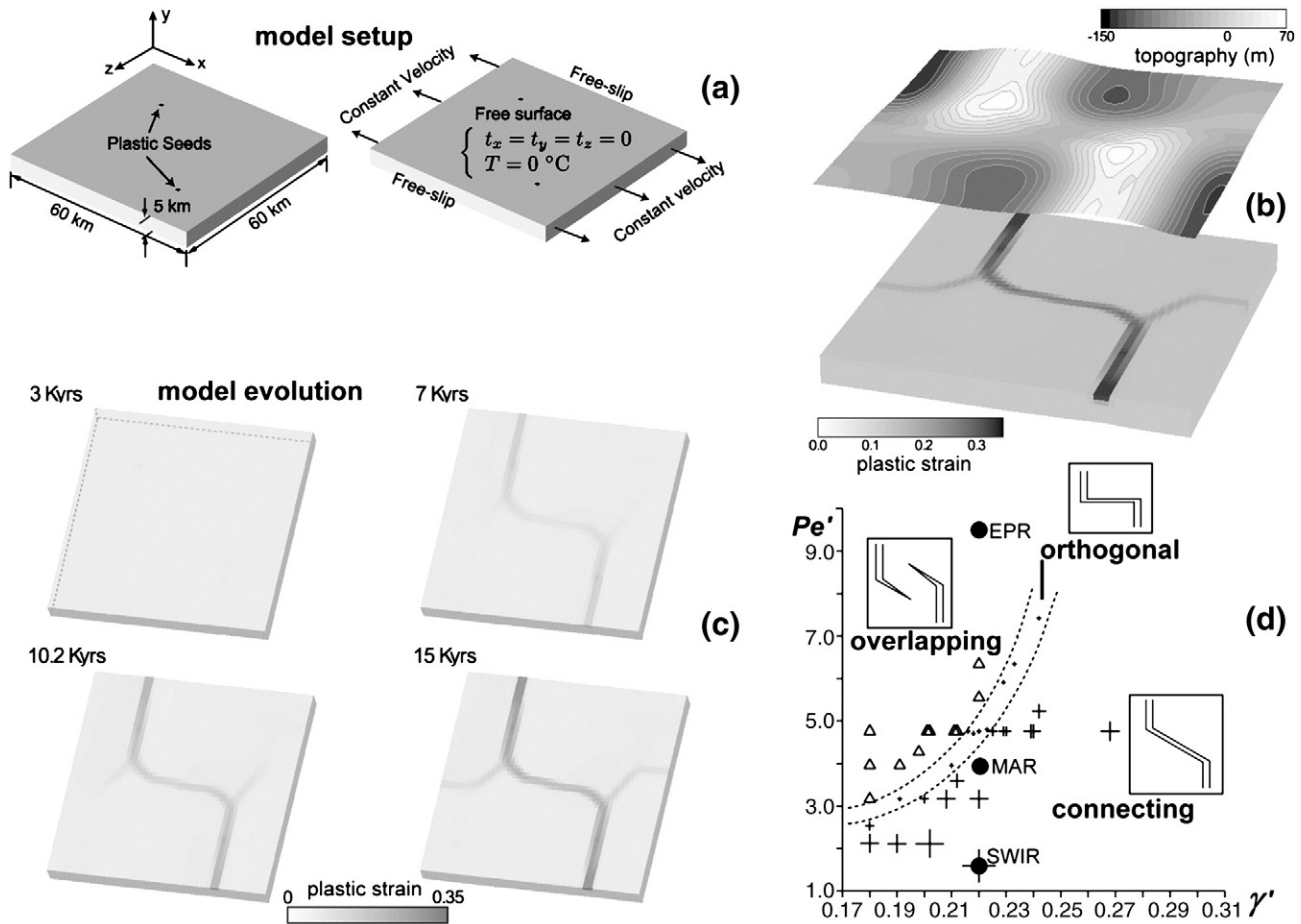


Fig. 10. 3D numerical experiments of Choi et al. (2008) on plate fragmentation with pre-existing ridge offset. (a) Model setup. (b) Model topography in case of an orthogonal ridge-transform fault pattern. (c) Development of the orthogonal pattern of plate fragmentation. (d) Summary of experimental results (symbols) and natural data (MAR = Mid Atlantic Ridge, EPR = East Pacific Rise, SWIR = Southwest Indian Ridge). Pe' is the spreading rate normalized by a reference cooling rate. γ' is the ratio of thermal stress to the reference spreading-induced stress.

spreading centers have small offsets suggests that distributed shear deformation is possible in thin, weak lithosphere near the ridge (Bell and Buck, 1992).

- At least three different mechanisms are required for the MOR system: tensile damage for ridge propagation, stress-induced shear damage for initially diffuse damage that gradually focuses into shear zones, and energy-induced shear damage that allows microplates to form and causes additional focusing of shear zones.
- A decreased tendency for ridge propagation (or an increased tendency for shear damage) results in 45° -connections between spreading segments observed at ultraslow ridges.
- The final geometry of the plate boundary is not a configuration of minimum strain energy or of minimal energy dissipation.

The work of Hieronymus (2004) demonstrated obvious advances in reproducing various spreading patterns observed in nature. These patterns appear in the model as the result of plate fragmentation process under condition of pre-existing ridge offset that remained constant through time. Indeed, spontaneous nucleation and growth of transform faults at single straight ridges (e.g., Menard and Atwater, 1968; Merkur'ev et al., 2009; Oldenburg and Brune, 1972) and changes of ridge offsets along transform faults with time (e.g., Sandwell, 1986; Stoddard and Stein, 1988) remained as a challenge. Among the conclusions from his study, Hieronymus (2004) proposed a need for more complete numerical model that includes spreading velocity and thickening of the cooling lithosphere.

Recently, first 3D numerical thermomechanical model of a spontaneous transform fault development by plate fragmentation was presented by Choi et al. (2008). In this study the mechanics responsible for the initiation of the orthogonal pattern characterizing mid-ocean ridges and transform faults were investigated in 3D with the use of an explicit Lagrangian finite difference method. The model (Fig. 10a) has an upper free surface and takes into account both thermal stresses arising from the cooling of young oceanic crust and extensional stresses arising from extensional kinematic boundary conditions imposed at two lateral boundaries. Thermal stress can exert ridge-parallel tension comparable in magnitude to spreading-induced tension when selectively released by ridges and ridge-parallel structure. Two modes of ridge segment growth have been identified in plan view: an overlapping mode where ridge segments overlap and bend toward each other and a connecting mode where two ridge segments are connected by an inclined transform-like fault. As the ratio of thermal stress to spreading-induced stress increases, the patterns of localized plastic strain change from the overlapping to connecting mode. The orthogonal pattern (Fig. 10b, c) marks the transition from one mode to the other (Fig. 10d). Besides the amount of stress from each driving force, the rate of stress accumulation is crucial in determining the emergent pattern. The obliquely connecting, the orthogonally connecting, and the overlapping mode are similar to ridge transform fault intersections observed in ultra-slow, slow to intermediate, and fast spreading centers, respectively. The patterns are also sensitive to the strain weakening rate. Fracture zones extending beside the transform faults (Fig. 10b) were also created in some models as a response to

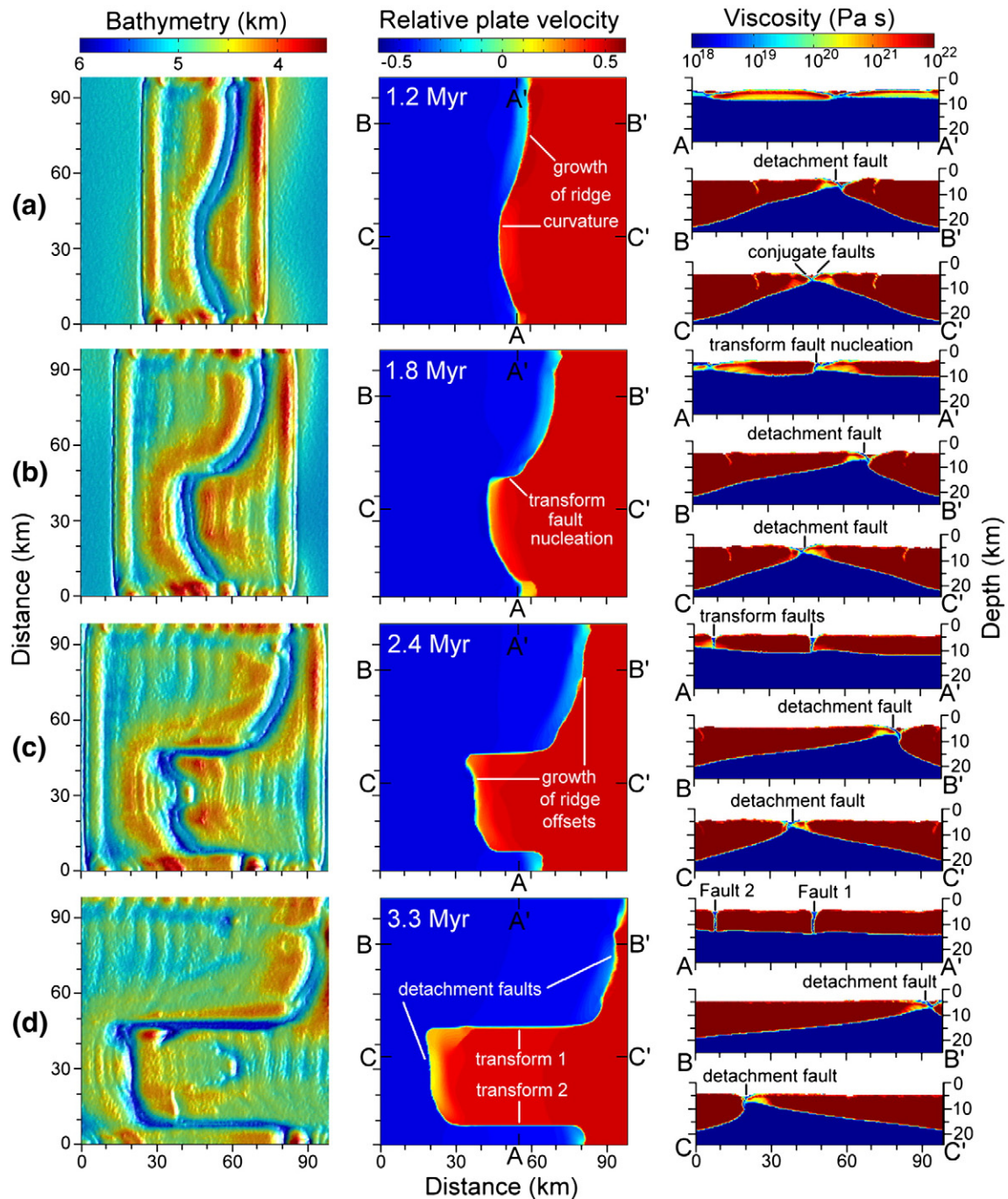


Fig. 11. 3D numerical experiments of Gerya (2010) showing spontaneous growth of transform faults at a single straight ridge. Sea level for bathymetry maps (left column) corresponds to the top of the model. Horizontal velocity in the middle column is normalized to the spreading rate. Diagrams in (a)–(d) show successive stages of the process at 1.2, 1.8, 2.4 and 3.3 Myr, respectively: (a) nucleation of ridge curvature; (b) nucleation of transform faults from the curved ridge sections; (c), (d) growth of ridge offsets along the transform faults.

thermal stress (Choi et al., 2008). It should be mentioned, however, that Choi et al. (2008) investigated the development of transform faults on the very short time scale of tens of thousands of years. Therefore, a long-term stability of developed patterns during subsequent plate accretion remained unknown.

Recently I performed a 3D numerical study of spontaneous transform faults nucleation and growth at single straight ridges (Gerya, 2010). This process was previously documented both in nature (e.g., Menard and Atwater, 1968; Merkur'ev et al., 2009) and in analog freezing wax models (Oldenburg and Brune, 1972, 1975) and required physical explanation. I documented results from high-resolution three-dimensional thermome-

chanical numerical models of the long-term plate spreading to investigate the physical conditions for the emergence of orthogonal ridge transform fault patterns. In contrast to previous numerical studies, the employed Eulerian–Lagrangian finite-difference, marker-in-cell model with open boundaries (Gerya, 2010) can model large strains and significant plate accretion. The modeled spreading rates range from 19 to 76 mm/yr (full rates) which simulates (ultra)slow- to intermediate-spreading ridges (e.g., Dick et al., 2003; Kriner et al., 2006; Small, 1998). Ridge geometries obtained in numerical experiments depend on model parameters and combine several tectonic elements such as straight and curved ridges, normal and detachment faults, ridge-orthogonal and oblique transform

faults, intra-transform spreading centers, and rotating microplates (Gerya, 2010).

Several models documented the spontaneous development of ridge-orthogonal transform faults from a single straight ridge (Fig. 11). At the initial stages of plate boundary evolution, the straight boundary is composed of two symmetrical conjugate normal faults along which deformation spontaneously localizes (Fig. 11a). Fracture-related weakening, implemented as a brittle/plastic strain weakening in the models, breaks the symmetry by partitioning extensional displacements between the two conjugate faults, as shown in previous 2D numerical experiments on lithospheric extension (Huismans and Beaumont, 2002). The choice of the dominating fault is random and depends

locally on small random perturbations of the initial temperature field. This choice can change along the ridge, thus producing lateral variation of asymmetric plate accretion and creating curvature of the ridge. After 1 million years, the plate boundary becomes gently curved in response to asymmetric plate growth that develops in alternate directions along successive ridge sections (Fig. 11a). Similar process was documented (Fig. 4b) in thermomechanical analog models of slow spreading (Shemenda and Grocholsky, 1994). Displacement along the dominant conjugate fault locally controls the asymmetric accretion of new lithosphere to the plates. The corresponding fault section gradually turns into a typical, upward convex detachment fault plane (cf. Fig. 11b and Fig. 4b). Such ridge-parallel detachment faults and asymmetric

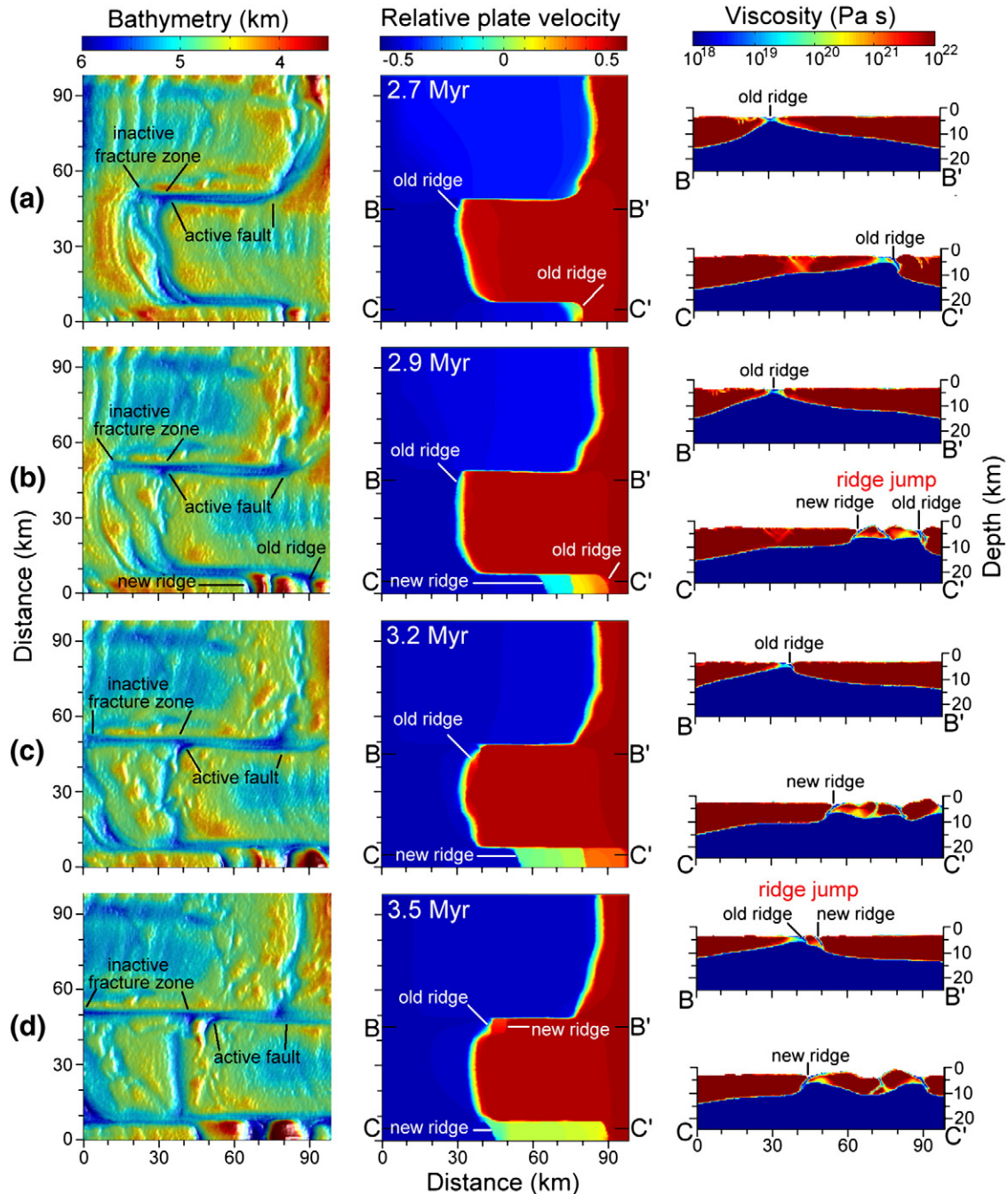


Fig. 12. Dynamics of development of inactive fracture zones after increase in the spreading rate (Gerya, 2010). Diagrams in (a)–(d) show successive stages of the process at 2.7, 2.9, 3.2 and 3.5 Myr, respectively: (a) stabilization of ridge offsets, nucleation of inactive fracture zones; (b)–(d) growth of inactive fracture zones, ridge jumps. Initial stages of model development correspond to Fig. 11a–c.

plate growth exist in relatively slow spreading ridges (e.g., Allerton et al., 2000; Collier et al., 1997; Escartin et al., 2008; Marks and Stock, 1995). The ridge curvature enhances with time (Figs. 11) leading to the emergence of transform faults along rotated ridge segments that became sub-parallel to the extension direction (Fig. 11b–d). Transform faults are thus initially nucleated as rotated and sheared sections of the mid-ocean ridge. The establishment of their vertical orientation occurs during the offset growth.

Numerical models suggest that transform faults are actively developing and result from dynamical instability of constructive plate boundaries. Boundary instability from asymmetric plate growth can spontaneously start in alternate directions along successive ridge sections; the resultant curved ridges become transform faults within a few million years. This dynamical instability has a rheological origin and can develop in the case of no gravity (Gerya, 2010). The instability is comparable to boudinage with the important difference that new material continuously adds to the stretched and rheologically strong lithospheric layer. The boundary instability is most efficient for the tested spreading rate of 38 to 57 mm/yr. Faster spreading rate of 76 mm/yr cause thinning of the plate contact and preclude the development of stable detachment faults, with symmetric plate growth and appearance of inactive fracture zones as a result (Fig. 12). For slower extension rates of 19 mm/yr, transform faults are ill-defined and deformation is dominated by growth and rotation of multiple blocks (microplates) and ridge-parallel rolls. This is consistent with analog models of slow spreading (Shemenda and Grocholsky, 1994) and with the lack of transform faults in ultraslow spreading ridges (Dick et al., 2003). Numerical experiments thus suggest that transform faults may preferably grow within a certain range of slow to intermediate spreading rates and mark an intermediate stage of plate separation between initial slow rifting and later steady spreading. This was prominent in one numerical experiment (Fig. 12) where the initial spreading rate of 38 mm/yr doubled after the appearance of transform faults (Fig. 11b). If the final spreading rate is high, symmetric growth will dominate and offsets of ridge segments may stabilize and inactive fracture zones may form at the flanks of the active transform faults (Fig. 12a–d).

Nucleation of transform faults strongly depends on the ridge orientation relative to the plate motion: A deviation of this orientation by 11 to 27° from perpendicular to spreading direction enhances the development of transform faults (Gerya, 2010). This suggests that after the transition from continental breakup to spreading (e.g., Taylor et al., 2009), transform faults will grow faster from initially inclined ridge sections. The ensuing pattern will thus reflect to some degree an original large-scale curvature of the rifted margin. This might explain the geometric correspondence between passive margins and mid-ocean ridges (e.g. Wilson, 1965). It also explains why transform faults develop rapidly at single straight ridges after a change in the spreading direction (e.g., Menard and Atwater, 1968; Merkur'ev et al., 2009).

Transform faults obtained in my numerical experiments (Figs. 11, 12) share similarities with natural observations. They are characterized by up to several km deep and wide topographic lows (DeMets et al., 2010; Gregg et al., 2007). Ridge offsets along the faults vary from tens to hundreds of km (DeMets et al., 2010; Fox and Gallo, 1984). Development of the faults occurs on the timescale of plate separation and thus should react nearly instantaneously to changes in spreading direction (Menard and Atwater, 1968; Merkur'ev et al., 2009). Curved ridges generated in numerical experiments are similar to some of the natural ridge structures (DeMets et al., 2010; Escartin et al., 2008; Gerya, 2010). They have a pronounced, often asymmetric axial valley characteristic of slow to intermediate spreading ridges [full spreading rates below 75–80 mm/yr (DeMets et al., 2010; Dick et al., 2003; Kriner et al., 2006; Small, 1998)]. Intra-transform spreading centers and hooked ridge tips produced by some numerical models (Gerya, 2010) are common in nature (e.g., DeMets et al., 2010). Nucleation and growth of transform faults in numerical models are associated with detachment faults and asymmetric accretion which are well documented in nature based on seismic and bathymetric data (Collier et al., 1997; Escartin et al., 2008; Marks and Stock, 1995). Modeled

asymmetric patterns of plate age distribution and changes of ridge offsets with time (Gerya, 2010) are indicated by magnetic data (Allerton et al., 2000; Stoddard and Stein, 1988).

Generally, my recent numerical experiments (Gerya, 2010) confirm results obtained in freezing wax models (e.g., O'Bryan et al., 1975; Oldenburg and Brune, 1972) and suggest that transform faults appear and grow gradually during the long-term plate accretion process from an arbitrary initial ridge configuration including single straight ridges. Consequently, the characteristic orthogonal ridge-transform fault pattern should be considered as a characteristic plate accretion pattern. This pattern does not correspond to the primary plate fragmentation (rifting) pattern that may have had completely different faults distribution and orientation (e.g., Taylor et al., 2009). The difference between these two alternative interpretations of an orthogonal ridge-transform fault pattern (i.e., plate accretion pattern vs. plate fragmentation pattern) is analogous to the difference between snowflakes (ice growth structures) and fragments of a thin broken ice plate (ice fragmentation structures).

Despite important advances in understanding several aspects of oceanic transform faults thermal structure, nucleation and mechanical behavior many first-order questions for their origination, stability and long-term evolution remain unanswered. Consequently, significant future efforts of numerical modeling community will unavoidably be directed toward further developing and applying of 3D thermomechanical numerical modeling approaches for transform faults.

5. Future modeling prospective

As can be seen from the previous section, numerical models of transform faults are yet relatively rare. This is mainly because of the intrinsic three-dimensionality and rheological complexity of the problem, which only recently became treatable with large-scale computing power. In contrast to freezing wax experiments in which various mid-ocean ridge-transform fault patterns formed during large plate divergence and growth (e.g., Katz et al., 2005; O'Bryan et al., 1975; Oldenburg and Brune, 1972, 1975; Ragnarsson et al., 1996; Shemenda and Grocholsky, 1994), most of numerical models focused on short-term/instantaneous processes such as thermal, flow, stress and displacement fields around kinematically prescribed transform faults (e.g., Behn et al., 2002, 2007; Forsyth and Wilson, 1984; Gregg et al., 2009; Gudmundsson, 1995; Hashima et al., 2008; Phipps Morgan and Forsyth, 1988) and fault patterns that arise from various thermo-mechanical loads on plates with pre-defined ridge offset (e.g., Choi et al., 2008; Hieronymus, 2004). These numerical experiments are consistent with analog modeling in that transform faults should be rheologically very weak (Behn et al., 2002); they also delineated conditions under which various fault patterns can nucleate from initially existing plate structure perturbations (Choi et al., 2008; Hieronymus, 2004). However, strain reached in majority of numerical experiments was too small to test the long-term stability of transform faults and investigate their spontaneous nucleation and growth in a self-consistent manner. On the other hand, single series of 3D numerical experiments conducted by myself for the processes of long-term accretion and spontaneous transform fault nucleation (Gerya, 2010) explored relatively simple inelastic plate model and neglected magmatic crust accretion (e.g., Buck et al., 2005). Consequently, a large number of open questions remain standing in relation to the origin of oceanic transform faults:

- What rheological mechanisms control nucleation, growth and long-term stability of oceanic transform faults and fracture zones?
- What controls geometry of mid-ocean ridges and spacing, offsets and orientation of transform faults?
- What controls geometry and dynamics of asymmetric accretion and detachment faults at mid-ocean ridges? What are relations between these structures and transform faults?

- What are possible geodynamic scenarios for past, present and future development of existing key natural oceanic ridge structures and which observables are most informative for predicting their dynamics?

Consequently, the following future modeling directions can be delineated:

- Conducting mutually coupled numerical and analog modeling experiments with the use of carefully modeled rheological properties of analog materials (e.g., [Buiter et al., 2006](#)) to understand main physical controls of nucleation and stability of transform faults in analog models and develop more robust rheological models of plates applicable to nature.
- Developing more realistic high-resolution 3D numerical models of mid-ocean ridges that include magmatic accretion of oceanic crust (e.g., [Buck et al., 2005](#)) and allows for spontaneous development of mid-ocean ridge-transform fault patterns (e.g., [Gerya, 2010](#)).
- Conducting systematic 3D experiments for understanding long-term evolution of various tectonic, topographic and crustal growth patterns found at mid-ocean ridges at a range of plate velocities from ultra-slow to ultra-fast (e.g., [Dick et al., 2003](#); [Kriner et al., 2006](#); [Small, 1998](#)).
- Performing numerical experiments for initiation and long-term development of mid-ocean ridge transform fault patterns following continental rifting and breakup. Understanding how and why gross-scale mid-ocean ridge geometries that are inherited from rifted continental margins (e.g., [Wilson, 1965](#)) can be maintained during millions of years of oceanic spreading.
- Conducting mutually coupled observational and numerical modeling studies (e.g., [Behn et al., 2007](#); [Gregg et al., 2009](#)) for existing key localities in ultraslow, slow, intermediate, fast and ultra-fast spreading ridges for which plate velocity measurements and high-resolution bathymetry data are available. Calibrating parameters of numerical models with natural data.

These lists are obviously non-exclusive and progress in modeling of oceanic transform faults will also require strong input from other disciplines (rheology, magmatic petrology, oceanography, seismology, geochemistry, numerical theory etc.). It also seems to be obvious that, due to an intrinsic physical complexity of oceanic spreading process, the role of realistic 3D numerical modeling approaches will inevitably grow providing an integrative basis for conducting quantitative cross-disciplinary mid-ocean ridge studies combining natural observations, analog experiments, and numerical modeling.

6. Summary and conclusions

Mid-ocean ridges sectioned by oceanic transform faults are one of the most prominent surface expressions of terrestrial plate tectonics. The perpendicularity of the ridges and the transform faults is an “intrinsic property” of most of the terrestrial oceanic spreading boundaries. A fundamental long standing problem of plate tectonics is how the orthogonal ridge transform fault pattern typical of spreading oceanic ridges has formed and why it is maintained. A number of key observations characterize oceanic transform faults in nature:

- They are found in a wide range of spreading velocities from 12–20 mm/yr to 145 mm/yr.
- Crustal structure and gravity signature in the regions of transform faults notably depend on the spreading rate of the ridge.
- Gross-scale geometry of mid-ocean ridge-transform fault patterns are often inherited from the patterns of respective rifted margins. Indeed, transform faults themselves seem to nucleate only after the beginning of the oceanic spreading.
- They can spontaneously form at a single straight ridge, particularly after changes in the spreading direction.

- Offsets along transform faults can change with time due to asymmetric plate accretion.
- There is a correlation between ridge segment length and spreading rate.
- Most of the slip along oceanic transform faults is accommodated by slow subseismic mechanisms, rather than the fast ruptures that dominate continental strike-slip faults.

Two main groups of analog models of transform faults were investigated: themomechanical (freezing wax) models with accreting and cooling plates and mechanical models with non-accreting brittle lithosphere. The following key features are observed:

Freezing wax models:

- Ridge-ridge transform faults, inactive fracture zones, rotating microplates, overlapping spreading centers and other features characteristic of spreading oceanic ridges can be produced in freezing wax experiments.
- The orthogonal pattern is a preferred mode of separation in waxes that produce notable anisotropy of crystallizing solid crust made of wax fibers that are oriented parallel to spreading direction.
- Orthogonal transform faults may form in a number of ways that involve development of overlapping spreading centers, viscous deformation of the crust and asymmetric/differential plate accretion and cooling.
- An orthogonal pattern in waxes may disintegrate when the spreading velocity is increased beyond some critical value.
- Asymmetric spreading, detachment faults and ridge jumps are observed in the case of slow spreading. The respective ridges can be strongly curved but the transform faults are not well pronounced.
- Open spreading centers with exposed liquid wax are often produced that does not preclude formation and stability of transform faults.

Non-accreting models:

- Intra-transform deformation pattern is controlled by the presence and width of a weak layer underneath/inside the transform.
- Ridges with smaller initial offsets develop interactions similar to overlapping spreading centers, whereas ridges with larger offsets produce geometries reminiscent of transform zones.

Numerical models of transform faults include both mechanical and themomechanical approaches. Three main types of model setups were investigated numerically: models of stress and displacement distribution around transforms, models of their thermal structure and crustal growth, and models of nucleation and evolution of ridge-transform fault patterns. The following key results and conclusions were obtained:

Stress and displacement distribution:

- Biaxial (ridge-parallel and ridge-perpendicular) tensile loading exists in the regions of transform faults. Least compressive stress direction becomes oblique to the spreading direction near the ridge-transform intersection.
- The occurrence of a strike-slip earthquake at the transform fault releases the distortion of the horizontal displacement field produced by the opening of the spreading centers in the interseismic period.
- On time scales longer than a typical earthquake cycle transform faults should behave as zones of significant weakness.

Thermal structure and crustal growth:

- Several kilometers of crustal thinning can plausibly occur within 30 km of transform faults at low to intermediate spreading rates. This thinning is due to perturbations in melt migration and production near a transform offset.
- Both the viscoplastic rheology and wide melt pooling are required to reproduce the observed variations in gravity inferred crustal thickness at intermediate and fast spreading ridges.

Nucleation and evolution:

- A limited number of fundamental spreading modes can form during fragmentation of elastic plate with pre-existing ridge offset: transform faults, microplates, overlapping spreading centers, zigzag ridges and oblique connecting spreading centers. The ratio of thermal stress to spreading-induced stress defines transition from overlapping to connecting mode. The orthogonal pattern marks the transition from one fragmentation mode to the other.
- Transform faults can form without initial ridge offsets at single straight ridges as a result of dynamical instability of accreting plate boundaries that operates on a million year timescale.
- The orthogonality of mid-ocean ridges and transform faults is established gradually by asymmetric plate accretion. This orthogonality is a characteristic plate accretion pattern that is generally dissimilar to initial plate fragmentation pattern.
- Zero-offset transforms can be generated by random asymmetric accretion along adjacent spreading centers. In contrast, very long transform faults cannot be generated by this process.

Both numerical and analog models of transform faults are still relatively scarce and a number of first order questions concerning the origin and evolution of these faults remain unanswered. Significant future cross-disciplinary efforts combining natural observations, analog experiments, and numerical modeling are needed.

Acknowledgments

J.-P. Burg is thanked for discussions and comments. This work was supported by ETH research grants ETH-0807-2, ETH-0807-3, ETH-0609-2, SNF research grants 200020-126832, 200020-129487, SNF ProDoc program 4-D-Adamello, TopoEurope Program and Crystal2Plate program. Constructive reviews from A. Gudmundsson and an anonymous reviewer are appreciated.

References

Abercrombie, R., Ekström, G., 2001. Earthquake slip on oceanic transform faults. *Nature* 410, 74–77.

Allerton, S., Escartin, J., Searle, R.C., 2000. Extremely asymmetric magmatic accretion of oceanic crust at the ends of slow-spreading ridge segments. *Geology* 28, 179–182.

Behn, M.D., Lin, J., 2000. Segmentation in gravity and magnetic anomalies along the U.S. east coast passive margin: implications for incipient structure of the oceanic lithosphere. *J. Geophys. Res.* 105, 25769–25790.

Behn, M.D., Lin, J., Zuber, M.T., 2002. Evidence for weak oceanic transform faults. *Geophys. Res. Lett.* 29. doi:10.1029/2002GL015612.

Behn, M.D., Boettcher, M.S., Hirth, G., 2007. Thermal structure of oceanic transform faults. *Geology* 35, 307–310.

Bell, R.E., Buck, W.R., 1992. Crustal control of ridge segmentation inferred from observations of the Reykjanes Ridge. *Nature* 357, 583–586.

Blackman, D.K., Forsyth, D.W., 1991. Isostatic compensation of tectonic features of the Mid-Atlantic Ridge: 25°–27°30' S. *J. Geophys. Res.* 96, 11741–11758.

Boettcher, M.S., Jordan, T.H., 2004. Earthquake scaling relations for mid-ocean ridge transform faults. *J. Geophys. Res.* 109, B12302.

Bonatti, E., 1996. Long-lived oceanic transform boundaries formed above mantle thermal minima. *Geology* 24, 803–806.

Brune, J.N., 1968. Seismic moment, seismicity, and rate of slip along major fault zones. *J. Geophys. Res.* 73, 777–784.

Buck, W.R., Lavier, L.L., Poliakov, A.N.B., 2005. Modes of faulting at mid-ocean ridges. *Nature* 434, 719–723.

Buiter, S.J.H., Babeyko, A.Yu., Ellis, S., Gerya, T.V., Kaus, B.J.P., Kellner, A., Schreurs, G., Yamada, Y., 2006. The numerical sandbox: comparison of model results for a shortening and an extension experiment. In: Buiter, S.J.H., Schreurs, G. (Eds.), *Analog and Numerical Modelling of Crustal-Scale Processes*: Geological Society, London, Special Publications, 253, pp. 29–64.

Canales, J.P., Detrick, R., Toomey, D.R., Wilcock, S.D., 2003. Segment-scale variations in the crustal structure of 150–300 kyr old fast spreading oceanic crust (East Pacific Rise, 8u15' N–10u5' N) from wide-angle seismic refraction profiles. *Geophys. J. Int.* 152, 766–794.

Chemenda, A., Deverchere, J., Calais, E., 2002. Three-dimensional laboratory modelling of rifting: application to the Baikal Rift, Russia. *Tectonophysics* 356, 253–273.

Choi, E., Lavier, L., Gurnis, M., 2008. Thermomechanics of mid-ocean ridge segmentation. *Phys. Earth Planet. Inter.* 171, 374–386.

Cochran, J.R., Martinez, F., 1988. Evidence from the northern Red Sea on the transition from continental to oceanic rifting. *Tectonophysics* 153, 25–53.

Collier, J.S., Danobeitia, J.J., CD82 Scientific Party, 1997. Evidence for asymmetric accretion and low-angle, planar faults in slow-spreading oceanic crust. *Geology* 25, 1075–1078.

Cox, A., 1973. *Plate Tectonics and Geomagnetic Reversals*. W. H. Freeman, San Francisco.

Dauteuil, O., Brun, J., 1993. Oblique rifting in a slow-spreading ridge. *Nature* 361, 145–148.

Dauteuil, O., Bourgeois, O., Mauduit, T., 2002. Lithosphere strength controls oceanic transform zone structure: insights from analogue models. *Geophys. J. Int.* 150, 706–714.

De Bremaecker, J.C., Swenson, D.V., 1990. Origin of overlapping spreading centers: a finite element study. *Tectonics* 9, 505–519.

DeMets, C., Gordon, R.G., Argus, D.F., 2010. Geologically current plate motions. *Geophys. J. Int.* 181, 1–80.

Dick, H.J., Lin, J., Schouten, H., 2003. An ultraslow-spreading class of ocean ridge. *Nature* 426 (6965), 405–412.

Engeln, J.F., Stein, S., Werner, J., Gordon, R.G., 1988. Microplate and shear zone models for oceanic spreading center reorganizations. *J. Geophys. Res.* 93, 2839–2856.

Escartin, J., Smith, D.K., Cann, J., Schouten, H., Langmuir, C.H., Escrig, S., 2008. Central role of detachment faults in accretion of slow-spreading oceanic lithosphere. *Nature* 455, 790–795.

Forsyth, D.W., Wilson, B., 1984. Three-dimensional temperature structure of a ridge-transform-ridge system. *Earth Planet. Sci. Lett.* 70, 355–362.

Fox, P.J., Gallo, D.G., 1984. A tectonic model for ridge-transform-ridge plate boundaries: implications for the structure of oceanic lithosphere. *Tectonophysics* 104, 205–242.

Freund, R., Merzer, A.M., 1976. Anisotropic origin of transform faults. *Science* 192, 137–138.

Froidevaux, C., 1973. Dissipation and geometric structure at spreading plate boundaries. *Earth Planet. Sci. Lett.* 20, 419–424.

Fujita, K., Sleep, N., 1978. Membrane stresses near mid-ocean ridge-transform intersections. *Tectonophysics* 50, 207–221.

Furlong, K.P., Sheaffer, S.D., Malservisi, R., 2001. Thermal-rheological controls on deformation within oceanic transforms. In: Holdsworth, R.E., et al. (Ed.), *The Nature and Tectonic Significance of Fault Zone Weakening*: Geological Society (London) Special Publication, 186, pp. 65–84.

Gerya, T., 2010. Dynamical instability produces transform faults at mid-ocean ridges. *Science* 329, 1047–1050.

Gregg, P.M., Lin, J., Behn, M.D., Montesi, L.G.J., 2007. Spreading rate dependence of gravity anomalies along oceanic transform faults. *Nature* 448, 183–187.

Gregg, P.M., Behn, M.D., Lin, J., Grove, T.L., 2009. Melt generation, crystallization, and extraction beneath segmented oceanic transform faults. *J. Geophys. Res.* 114, B11102.

Gudmundsson, A., 1995. Stress fields associated with oceanic transform faults. *Earth and Planet. Sci. Lett.* 136, 603–614.

Gudmundsson, A., 2007. Infrastructure and evolution of ocean-ridge discontinuities in Iceland. *J. Geodyn.* 43, 6–29.

Hashima, A., Takada, Y., Fukahata, Y., Matsu'ura, M., 2008. General expressions for internal deformation due to a moment tensor in an elastic/viscoelastic multilayered half-space. *Geophys. J. Int.* 175, 992–1012.

Hey, R.N., Johnson, P.D., Martinez, F., Korenaga, J., Somers, M.L., Huggett, Q.J., LeBas, T.P., Rusby, R.L., Naar, D.F., 1995. Plate boundary reorganization at a large-offset rapidly propagating rift. *Nature* 378, 167–170.

Hieronymus, C.F., 2004. Control on seafloor spreading geometries by stress- and strain-induced lithospheric weakening. *Earth Planet. Sci. Lett.* 222, 177–189.

Huismans, R.S., Beaumont, C., 2002. Asymmetric lithospheric extension: the role of frictional-plastic strain softening inferred from numerical experiments. *Geology* 30, 211–214.

Ihmlé, P.F., Jordan, T.M., 1994. Teleseismic search for slow precursors to large earthquakes. *Science* 266, 1547–1551.

Ihmlé, P.F., Harabaglia, P., Jordan, T.H., 1979. Teleseismic detection of a slow precursor to the great 1989 Macquarie Ridge earthquake. *Science* 261, 177–183.

Kanamori, H., Stewart, G.S., 1976. Mode of the strain release along the Gibbs fracture zone. *Mid-Atl. Ridge. Phys. Earth Planet. Inter.* 11, 312–332.

Karson, J., Dick, H., 1983. Tectonics of ridge-transform intersections at the Kane fracture zone. *Mar. Geophys. Res.* 6, 51–98.

Katz, R.F., Ragnarsson, R., Bodenschatz, E., 2005. Tectonic microplates in a wax model of sea-floor spreading. *New J. Phys.* 7. doi:10.1088/1367-2630/7/1/037.

Kinzler, R.J., Grove, T.L., 1992a. Primary magmas of mid-ocean ridge basalts: 1. Experiments and methods. *J. Geophys. Res.* 97, 6885–6906.

Kinzler, R.J., Grove, T.L., 1992b. Primary magmas of mid-ocean ridge basalts: 2. Applications. *J. Geophys. Res.* 97, 6907–6926.

Kinzler, R.J., Grove, T.L., 1993. Corrections and further discussion of the primary magmas of mid-ocean ridge basalts, 1 and 2. *J. Geophys. Res.* 98, 22,339–22,347.

Criner, K.A., Pockalny, R.A., Larson, R.L., 2006. Bathymetric gradients of lineated abyssal hills: inferring seafloor spreading vectors and a new model for hills formed at ultra-fast rates. *Earth and Planet. Sci. Lett.* 242, 98–110.

- Kuo, B.Y., Forsyth, D.W., 1988. Gravity anomalies of the ridge transform intersection system in the South Atlantic between 31 and 34.5°S: upwelling centers and variations in crustal thickness. *Mar. Geophys. Res.* 10, 205–232.
- Lin, J., Phipps Morgan, J., 1992. The spreading rate dependence of three-dimensional mid-ocean ridge gravity structure. *Geophys. Res. Lett.* 19, 13–16.
- Lin, J., Purdy, G.M., Schouten, H., Sempere, J.-C., Zervas, C., 1990. Evidence from gravity data for focused magmatic accretion along the Mid-Atlantic Ridge. *Nature* 344, 627–632.
- Macdonald, K.C., Fox, P.J., Perram, L.J., Eisen, M.F., Haymon, R.M., Miller, S.P., Carbotte, S.M., Cormier, M.-H., Shor, A.N., 1988. A new view of the mid-ocean ridge from the behavior of ridge-axis discontinuities. *Nature* 335, 217–225.
- Macdonald, K., Scheirer, D., Carbotte, S., 1991. Mid-ocean ridges: discontinuities, segments and giant cracks. *Science* 253 (5023), 986–994.
- Marks, K.M., Stock, J.M., 1995. Asymmetric seafloor spreading and short ridge jumps in the Australian-Antarctic Discordance. *Mar. Geophys. Res.* 17, 361–373.
- Marques, F.O., Cobbold, P.R., Lourenço, N., 2007. Physical models of rifting and transform faulting, due to ridge push in a wedge-shaped oceanic lithosphere. *Tectonophysics* 443, 37–52.
- Mauduit, T., Dauteuil, O., 1996. Small-scale models of oceanic transform zones. *J. Geophys. Res.* 101, 20195–20209.
- McClay, K., Khalil, S., 1998. Extensional hard linkages, eastern Gulf of Suez, Egypt. *Geology* 26, 563–566.
- McGuire, J.J., Ihmle, P.F., Jordan, T.H., 1996. Time domain observations of a slow precursor to the 1994 Romanche transform earthquake. *Science* 274, 82–85.
- Menard, H.W., 1967. Sea-floor spreading, topography, and the second layer. *Science* 157, 923–924.
- Menard, H.W., Atwater, T., 1968. Changes in direction of seafloor spreading. *Nature* 219, 463–467.
- Merkur'ev, S.A., DeMets, C., Gurevich, N.I., 2009. Geodynamic evolution of crust accretion at the axis of the Reykjanes ridge, Atlantic ocean. *Geotectonics* 43, 194–207.
- Naar, D.F., Hey, R.N., 1989. Speed limit for oceanic transform faults. *Geology* 17, 420–422.
- O'Bryan, J.W., Cohen, R., Gilliland, W.N., 1975. Experimental origin of transform faults and straight spreading-center segments. *GSA Bull.* 86, 793–796.
- Okal, E.A., Stewart, L.M., 1992. Slow earthquakes along oceanic fracture zones: evidence for asthenospheric flow away from hotspots? *Earth Planet. Sci. Lett.* 57, 75–87.
- Oldenburg, D.W., Brune, J.N., 1972. Ridge transform fault spreading pattern in freezing wax. *Science* 178, 301.
- Oldenburg, D.W., Brune, J.N., 1975. An explanation for the orthogonality of ocean ridges and transform faults. *J. Geophys. Res.* 80, 2575–2585.
- Phipps Morgan, J., Forsyth, D.W., 1988. Three-dimensional flow and temperature perturbations due to a transform offset: effects on oceanic crust and upper mantle structure. *J. Geophys. Res.* 93, 2955–2966.
- Phipps Morgan, J., Parmentier, E., 1984. Lithospheric stress near a ridge transform intersection. *Geophys. Res. Lett.* 11, 113–116.
- Ragnarsson, R., Ford, J.L., Santangelo, C.D., Bodenschatz, E., 1996. Rifts in spreading wax layers. *Phys. Rev. Lett.* 76, 3456–3459.
- Reichle, M.S., Sharman, G.F., Brune, J.N., 1976. Sonobuoy and teleseismic study of Gulf of California. Transform fault earthquake sequences. *Bull. Seismol. Society Am.* 66, 1623–1641.
- Rundquist, D.V., Sobolev, P.O., 2002. Seismicity of mid-oceanic ridges and its geodynamic implications: a review. *Earth-Sci. Rev.* 58, 143–161.
- Sandwell, D., 1986. Thermal stress and the spacings of transform faults. *J. Geophys. Res.* 91, 6405–6417.
- Schouten, H., Klitgord, K.D., Gallow, D.G., 1993. Edge-driven microplate kinematics. *J. Geophys. Res.* 98, 6689–6701.
- Sempere, J., Macdonald, K.C., 1986. Overlapping spreading centers: implications from crack growth simulation by the displacement discontinuity method. *Tectonics* 5, 151–163.
- Shemenda, A.I., Grocholsky, A.L., 1994. Physical modeling of slow seafloor spreading. *J. Geophys. Res.* 99, 9137–9153.
- Shen, Y., Forsyth, D.W., 1992. The effects of temperature- and pressure dependent viscosity on three-dimensional passive flow of the mantle beneath a ridge-transform system. *J. Geophys. Res.* 97, 19,717–19,728.
- Shouten, H., White, R.S., 1980. Zero offset fracture zones. *Geology* 8, 175–179.
- Small, C., 1998. Global systematics of mid-ocean ridge morphology. In: Buck, W., Delaney, P.T., Karson, J.A., Lagabriele, Y. (Eds.), *Faulting and Magmatism at Mid-Ocean Ridges*. American Geophysical Union, Washington D.C., pp. 1–26.
- Sparks, D.W., Parmentier, E.M., 1991. Melt extraction from the mantle beneath spreading centers. *Earth Planet. Sci. Lett.* 105, 368–377.
- Stoddard, P.R., Stein, S., 1988. A kinematic model of ridge-transform geometry evolution. *Mar. Geophys. Res.* 10, 181.
- Taylor, B., Goodliffe, A., Martinez, F., 2009. Initiation of transform faults at rifted continental margins. *C. R. Geosci.* 341, 428.
- Tentler, T., 2003a. Analogue modeling of tension fracture pattern in relation to mid-ocean ridge propagation. *Geophys. Res. Lett.* 30, 1268.
- Tentler, T., 2003b. Analogue modeling of overlapping spreading centers: insights into their propagation and coalescence. *Tectonophysics* 376, 99–115.
- Tentler, T., 2007. Focused and diffuse extension in controls of ocean ridge segmentation in analogue models. *Tectonics* 26, TC5008.
- Tentler, T., Accolla, V., 2010. How does the initial configuration of oceanic ridge segments affect their interaction? Insights from analogue models. *J. Geophys. Res.* 115, B01401.
- Tolstoy, M., Harding, A., Orcutt, J., 1993. Crustal thickness on the Mid-Atlantic Ridge: bulls-eye gravity anomalies and focused accretion. *Science* 262, 726–729.
- Watts, A.B., Stewart, J., 1998. Gravity anomalies and segmentation of the continental margin offshore West Africa. *Earth Planet. Sci. Lett.* 156, 239–252.
- Wilson, J.T., 1965. A new class of faults and their bearing on continental drift. *Nature* 207, 343–347.
- Winterer, E.L., 1976. Anomalies in the tectonic evolution of the Pacific. In: Sutton, G.S., Manghnani, M.H., Moberly, R. (Eds.), *The Geophysics of the Pacific Ocean Basin and its Margin*, *Geophys. Monogr. Ser.*, vol. 19. AGU, Washington D. C, pp. 269–280.